Hindawi
Journal of Nanomaterials
Volume 2024, Article ID 5482168, 20 pages
https://doi.org/10.1155/2024/5482168

Research Article

Computation of Structural Descriptors of Pyrene Cored Dendrimers through Quotient Graph Approach and Its Graph Entropy Measures

D. Antony Xavier,[1] **Annmaria Baby**,[1] **Ammar Alsinai**,[2] **Eddith Sarah Varghese**,[1] **and Hanan Ahmed**[3]

[1]*Department of Mathematics, Loyola College, University of Madras, Chennai, India*
[2]*Department of Mathematics, University of Mysore, Mysuru, India*
[3]*Department of Mathematics, Ibb University, Ibb, Yemen*

Correspondence should be addressed to Hanan Ahmed; hananahmed1a@gmail.com

Received 22 November 2022; Revised 2 February 2024; Accepted 7 February 2024; Published 16 February 2024

Academic Editor: Jeyadevan Balachandran

Dendrimers are highly defined hyperbranched artificial macromolecules, synthesised by convergent or divergent approach with specific applications in various fields. Dendrimers can be represented as graph models, from which a quantitative description can be drawn in relation with their structural properties. The distance-based and the degree-based descriptors have great importance and huge applications in structural chemistry. These indices together with entropy measures are found to be more effective and have found application in scientific fields. The idea of graph entropy is to characterise the complexity of graphs. The use of these graph invariants in quantitative structure property relationship and quantitative structure activity relationship studies has become of major interest in recent years. In this paper, the distance-based molecular descriptors of pyrene cored dendrimers are studied applying the technique of converting original graph into quotient graphs using Θ^*-classes. It is to be noted that, since the pyrene cored dendrimer, Gn is not a partial cube, usual cut method is not applicable. Further, various degree-based descriptors and their corresponding graph entropies of the pyrene cored dendrimers are also studied. Based on the obtained results, a comparative analysis as well as a regression analysis was carried out.

1. Introduction

Dendrimers are highly defined hyperbranched artificial macromolecules that represent a class of novel polymers. These molecules were discovered by Fritz Vogtle in 1978, Tomalia et al. [1] in the early 1980s and George R. Newkome during the same period but independently [1, 2]. They feature distinct 3D molecular architectures with well-defined structures that include three different units: the central core, dendrons, and terminal functional group. The core is surrounded by dendron layers known as generations or branches that extend outward and terminate with surface groups. Over the last few decades, a variety of dendrimers have been synthesised using either a convergent or divergent approach, with specialised uses in a variety of sectors [3]. Dendrimers have a compact and globular structure, a spherical shape, a regular architecture, and develop in a stepwise manner. These structures are non-crystalline and amorphous with lower glass temperatures. They also have high aqueous solubility, high nonpolar solubility and low compressibility. These qualities and properties distinguish dendrimer from linear or branching polymers [4]. Their high degree of molecular uniformity and low polydispersity make them attractive materials for the development of nanomedicines [5]. They also have applications in drug delivery [6, 7], material science and biology [8], magnetic resonance imaging [9], homogeneous catalysis, optical data storage, solar cells, science and engineering, organic light-emitting device, and so on [10, 11]. The dendrimer chemistry provides an effective tool for tuning the properties of the dendrimers by altering the core or tailoring the size, chemical, and topological structures of the dendrons [11]. The proper core selection and detailed design of dendrons are essential for the final attributes of a dendrimer.

Table 1: Distance-based indices of strength-weighted graph $G_{sw} = G$.

Distance-based index	Mathematical formula
Wiener [34]	$W(G) = \sum_{\{p,q\} \subseteq V(G)} w_v(p) w_v(q) d_G(p,q)$
Szeged [34]	$Sz_v(G) = \sum_{g=pq \in E(G)} s_e(g) n_p(g\|G) n_q(g\|G)$
Edge Szeged [34]	$Sz_e(G) = \sum_{g=pq \in E(G)} s_e(g) m_p(g\|G) m_q(g\|G)$
Padmakar–Ivan [34]	$\mathrm{PI}(G) = \sum_{g=pq \in E(G)} s_e(g) [m_p(g\|G) + m_q(g\|G)]$
Mostar [35]	$\mathrm{Mo}(G) = \sum_{g=pq \in E(G)} s_e(g) \|n_p(g\|G) - n_q(g\|G)\|$
Edge Mostar [35]	$\mathrm{Mo}_e(G) = \sum_{g=pq \in E(G)} s_e(g) \|m_p(g\|G) - m_q(g\|G)\|$

Pyrene, a polycyclic aromatic hydrocarbon consisting of four fused benzene rings is a fascinating core for constructing light-emitting dendrimers. Carbazole is a luminescence compound with high hole-transporting ability arising from the lone pair electrons in nitrogen atom and have been incorporated as dendrons to construct dendrimer materials [12]. The combination of pyrene and carbazole is expected to provide improved thermal stability and good charge-transportation ability. Three generations of dendrimers $G1$, $G2$, and $G3$ with a pyrene core and 9-phenylcarbazole derivatives dendrons designed and synthesised by convergent approach were reported by You et al. [11, 12]. These dendrimers exhibit high thermal stability and has the potential to be employed in optoelectronic applications [11]. Also, Gingras et al. [13] synthesised and characterised a new class of dendrimers $PyG0$, $PyG1$, and $PyG2$, called polysulfurated pyrene dendrimers consisting of a polysulfurated pyrene core with appended thiophenylene units. These dendrimers exhibit remarkable photophysical and redox properties [14].

A topological index is a numerical number associated with a graph that is related to the graph's structural characteristics. Chemical structures can be represented as graph models and can be assigned with these numerical values, which are associated with the physical, chemical, and biological properties of the structure. Hence, the graph models may be utilised to investigate different aspects of the relevant chemical structure. In 1947, chemist Wiener [15] developed the Wiener index, the first molecular descriptor. Many additional molecular descriptors were added, each of which corresponds to a particular property of the chemical structure. The distance- and degree-based indices are generally recognised because of their numerous applications in structural chemistry. In recent years, there has been a lot of interest in using these graph invariants in quantitative structure–property relationships (QSPR) and quantitative structure–activity relationships (QSAR) research. They have also found application in various areas of chemistry, informatics, biology, etc. [15–22].

The concept of information entropy was first presented by Shannon [23] in order to analyse and quantify the complexity of data and information transmission. An important application of information entropy is to study the complexity and the quantum chemical electron densities of molecular structures [24]. Later Rasheysky introduced the idea of graph entropy in 1955 to characterise the complexity of graphs [25, 26]. The two categories of entropies are deterministic and probabilistic. The probabilistic method is applicable in characterising a chemical structure and it is classified into intrinsic and extrinsic, in which we determine the extrinsic measure. In intrinsic measures, a graph is partitioned into components sharing similar structures and a probability distribution is found over those components and in extrinsic measures, a probability function is assigned to elements of the graph, the vertices, or edges [27].

Table 2: Degree-based indices of graph G.

Degree-based index	Mathematical formula
First Zagreb [36]	$M_1(G) = \sum_{pq \in E(G)} (d_p + d_q)$
Second Zagreb [36]	$M_2(G) = \sum_{pq \in E(G)} (d_p \times d_q)$
Harmonic [37]	$H(G) = \sum_{pq \in E(G)} \frac{2}{d_p + d_q}$
Hyper Zagreb [38]	$HM(G) = \sum_{pq \in E(G)} (d_p + d_q)^2$
Forgotten [39]	$F(G) = \sum_{pq \in E(G)} ((dp)^2 + (d_q)^2)$
Randić [20]	$R(G) = \sum_{pq \in E(G)} \frac{1}{\sqrt{d_p \times d_q}}$
Reciprocal Randić [40]	$RR(G) = \sum_{pq \in E(G)} \sqrt{d_p \times d_q}$
Sum-connectivity [41]	$SC(G) = \sum_{pq \in E(G)} \frac{1}{\sqrt{d_p + d_q}}$
Geometric arithmetic [42]	$GA(G) = \sum_{pq \in E(G)} \frac{2\sqrt{d_p \times d_q}}{d_p + d_q}$
Atom bond connectivity [43]	$ABC(G) = \sum_{pq \in E(G)} \frac{\sqrt{d_p + d_q - 2}}{\sqrt{d_p \times d_q}}$
Irregulaity measure [44]	$irr(G) = \sum_{pq \in E(G)} \|d_p - d_q\|$
Sigma [45]	$\sigma(G) = \sum_{pq \in E(G)} (d_p - d_q)^2$

The topological indices of various dendrimers were studied in the past few years [28–33]. In this paper, the distance-based indices defined in Table 1 are studied for the pyrene cored dendrimers $Gn : n \geq 1$ and $PyGn : n \geq 0$, where n is the generation of the dendrimer. The various degree-based indices given in Table 2, and their corresponding graph entropies are also studied for the structures, see [46–50] for more recent papers in this field. The chemical applicability of these works is widely recognised by researchers and scientists. This motivated many reseachers in studying the concept of topological indices of chemical structures, see [51–61] for applications of chemical graph theory in various fileds. The structure of pyrene cored dendrimers $G2$ and $PyG2$ are given in Figure 1.

2. Mathematical Terminologies

Consider a simple, finite, connected graph G with vertex set, $V(G)$ and edge set, $E(G)$. The number of edges connected to a vertex p is the degree of vertex p, denoted by d_p. For more basic terminologies and definitions refer to [34, 62].

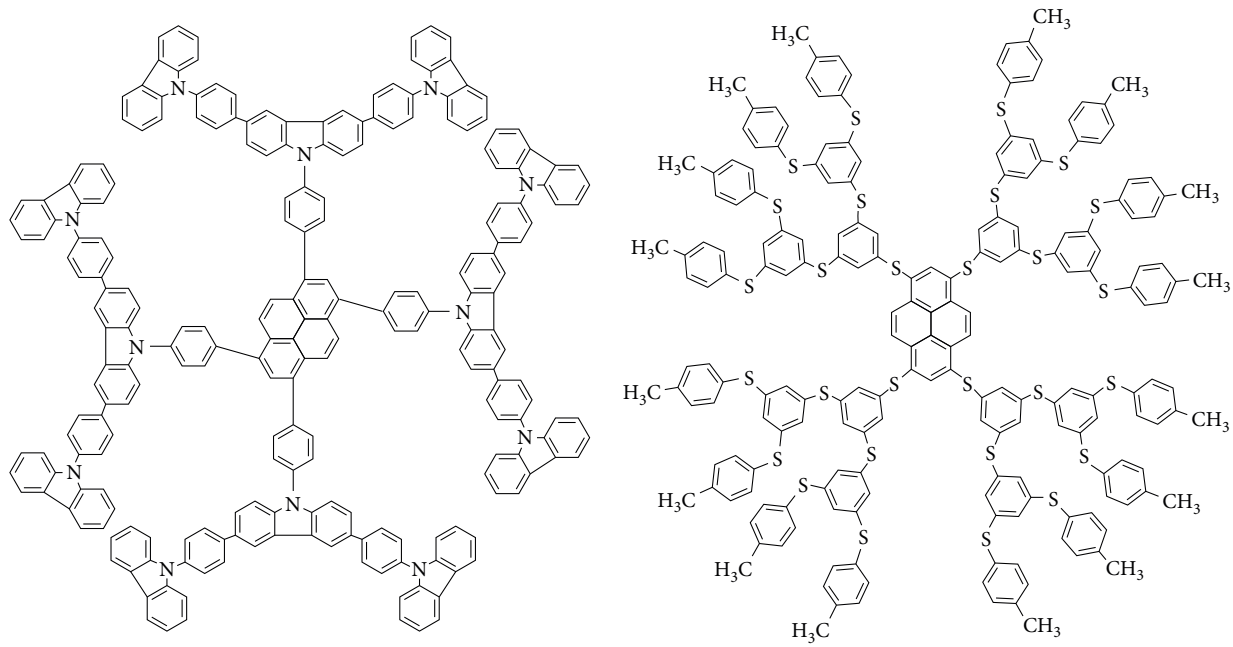

G2 *PyG2*

Figure 1: Second-generation pyrene cored dendrimer, *G*2, and second-generation polysulfurated pyrene dendrimer, *PyG*2.

For an edge $g = pq \in E(G)$,
$N_p(g|G) = \{x \in V(G) : d_G(p, x) < d_G(q, x)\}$, and
$M_p(g|G) = \{y \in E(G) : d_G(p, y) < d_G(q, y)\}$.

The cardinality of the sets $N_p(g|G)$ and $M_p(g|G)$ are denoted as $n_p(g|G)$ and $m_p(g|G)$, respectively. The values of $n_q(g|G)$ and $m_q(g|G)$ are analogous. The strength weighted graph denoted by $G_{sw} = (G, [w_v, s_v], s_e)$, where w_v is the vertex weight, s_v is the vertex strength, and s_e is the edge strength was presented by Arockiaraj et al. [34]. And the sets $N_p(g|G_{sw}) = N_p(g|G)$ and $M_p(g|G_{sw}) = M_p(g|G)$ are described with cardinality:

$$\begin{aligned} n_p(g|G_{sw}) &= \sum_{x \in N_p(g|G_{sw})} w_v(x) \text{ and } m_p(g|G_{sw}) \\ &= \sum_{x \in N_p(g|G_{sw})} s_v(x) + \sum_{y \in M_p(g|G_{sw})} s_e(y). \end{aligned} \tag{1}$$

The values of $n_q(g|G_{sw})$ and $m_q(e|G_{sw})$ are analogous.

The Djoković–Winkler (Θ) relation plays a major role in computing topological indices, which is defined as $d_G(q, b) + d_G(p, a) \neq d_G(p, b) + d_G(q, a)$, for two edges $g = pq$ and $f = ab$ of G. The relation Θ is reflexive, symmetric, and transitive in the case of partial cubes. Its transitive closure Θ^* forms an equivalence relation in general and partitions the edge set into convex components. Let $F = \{F_1, F_2, \ldots, F_r\}$ be the Θ^* equivalence class. A partition $\mathbb{E} = \{E_1, E_2, \ldots, E_k\}$ of $E(G)$ is said to be coarser than partition F if each set E_i is the union of one or more Θ^*-classes of G.

To determine the entropy measures, we have followed Shannon's model. In communication and transmission of information, each elements of the information are assigned with the probability functions in the form of symbols $x_1, x_2, \ldots, x_n$. If N_i denotes the number of times x_i appear in the information and N denotes the total length of information, then the Shannon's original information entropy measure, denoted by h is defined as follows [24]:

$$h = -\sum_{i=1}^{n} p_i \log(p_i), \text{ where } p_i = \frac{N_i}{N}. \tag{2}$$

In chemical graphs, the elements are the edges of the graph to which the probability function is assigned using the topological indices. If $\mathrm{TI}(G)$ denotes the topological index of G, then in general:

$$\mathrm{TI}(G) = \sum_{g \in E(G)} t(g), \tag{3}$$

where $t(g)$ is the functional characterisation of the topological index.

For example, if we consider the first Zagreb index, then the functional $t(g) = d_p + d_q$.

The graph entropy measure is denoted by $\mathrm{ENT}_{\mathrm{TI}}(G)$ and is defined as follows [24, 48, 63]:

$$\begin{aligned} \mathrm{ENT}_{\mathrm{TI}}(G) &= -\sum_{g \in E(G)} p_g \log\left(p_g\right), \\ \text{where } p_g &= \frac{t(g)}{\sum_{g \in E(G)} t(g)} = \frac{t(g)}{\mathrm{TI}(G)}. \end{aligned} \tag{4}$$

Therefore, $$\mathrm{ENT}_{\mathrm{TI}}(G) = \log(\mathrm{TI}(G)) - \frac{1}{\mathrm{TI}(G)} \sum_{g \in E(G)} t(g) \log(t(g)). \tag{5}$$

3. Distance-Based Topological Descriptor

In this section, we compute the distance-based indices for the pyrene cored dendrimers. For the computation, the original graph is transformed into smaller weighted graphs called as quotient graphs, for which the indices are computed in order to determine the indices of the original graph. The transformation to quotient graphs is carried out using the coarser partition set of Θ^*-classes of the graph. This technique is adopted, since the chemical graphs of Gn are not partial cubes, see [64–66] for more details regarding quotient graph approach.

k-rooted product of graphs G and H, denoted by Go_kH is the graph obtained by joining the root nodes of k copies of H to each vertex of G.

Theorem 1 (see [67]). *Let $G = K_1 o_m H$ be a connected weighted graph, and let h_i be the root nodes of H_i, where $H_i \cong H_j$, $i \in [m]$; $m \geq 2$. Then:*

$$W(G,w) = mW(H) + m(m-1) \sum_{x \in V(H_1)} \sum_{y \in V(H_2)} w(x)w(y) + \sum_{x \in V(H_1)} w(x) \left\{ m\, w(e) d(e,x) + \frac{m(m-1)}{2} \sum_{y \in V(H_2)} w(y)(d(h_2,y) + d(x,h_1)) \right\}, \tag{6}$$

where $e \in V(K_1)$.

Theorem 2. *For $n \geq 1$:*

$W(Gn) = (115{,}126 - 11{,}628n) \times 2^n + (51{,}984n - 84{,}246) \times 2^{2n} - 30{,}518$,

$Sz_v(Gn) = (214{,}786 - 19{,}304n) \times 2^n + (98{,}192n - 158{,}726) \times 2^{2n} - 55{,}052$,

$Sz_e(Gn) = (327{,}218 - 27{,}692n) \times 2^n + (143{,}888n - 241{,}638) \times 2^{2n} - 84{,}692$,

$\mathrm{PI}(Gn) = 8{,}096 \times 2^{2n} - 12{,}924 \times 2^n + 5{,}136$,

$\mathrm{Mo}(Gn) = 6{,}688 \times 2^{2n} - (2{,}660n + 7{,}768) \times 2^n + 1{,}192$,

$\mathrm{Mo}_e(Gn) = 8{,}096 \times 2^{2n} - (3{,}220n + 9{,}360) \times 2^n + 1{,}412$.

Proof. The molecular graph Gn has $76 \times 2^n - 60$ vertices, $92 \times 2^n - 73$ edges and $40 \times 2^n - 33$ Θ^*-classes. Let us consider $G2$. The sets E_i, which is coarser than the Θ^*-classes chosen for $G2$ are highlighted in Figure 2. We convert the original graph into quotient graphs Gn/E_i and we obtain $2n+1$ quotient graphs for Gn. There are three types of quotient graphs $\{Gn/E_1, Gn/E_{2i}, Gn/E_{2i+1} : 1 \leq i \leq n\}$ for Gn.

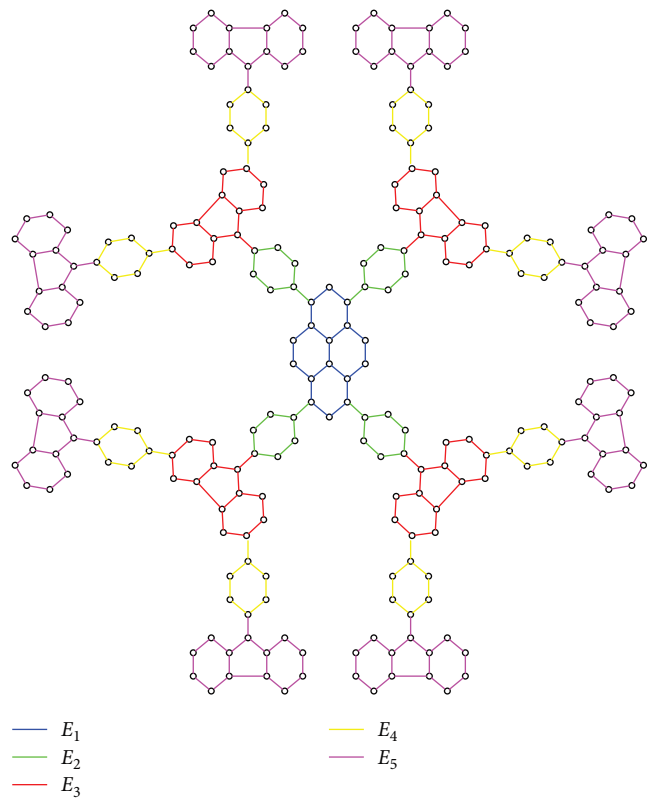

Figure 2: Illustration of sets E_i chosen for $G2$.

The first type of quotient graph Gn/E_1 has 16 vertices and 19 edges, among which four vertices, $a_j : 1 \leq j \leq 4$ has $(w_v(a_j), s_v(a_j)) = (19 \times 2^n - 18, 23 \times 2^n - 23)$ and for the remaining vertices, vertex weight is 1 and vertex strength is 0, as given in Figure 3.

The second type of quotient graph $Gn/E_{2i} : 1 \leq i \leq n$ has a weighted core vertex, say c attached with $m = 2^{i+1} : 1 \leq i \leq n$ branches such that one vertex in each branch has same weighted values as given in Figure 4. Let us take those vertices to be $b_k : 1 \leq k \leq m$. Then,

$(w_v(c), s_v(c)) = (38 \times 2^i - 60, 46 \times 2^i - 73)$,

$(w_v(b_k), s_v(b_k)) = (19 \times 2^{n-i+1} - 24, 23 \times 2^{n-i+1} - 30)$.

For the remaining vertices, vertex weight and vertex strength is 1 and 0, respectively.

The third type of quotient graph $Gn/E_{2i+1} : 1 \leq i \leq n$ has a weighted core vertex, say f attached with $m = 2^{i+1} : 1 \leq i \leq n$ branches such that two vertices in each branch has same weighted values as given in Figure 5. Those vertices are $d_r : 1 \leq r \leq 2m$. Then,

$(w_v(f), s_v(f)) = (50 \times 2^i - 60, 60 \times 2^i - 73)$,

$(w_v(d_r), s_v(d_r)) = (19 \times 2^{n-i} - 18, 23 \times 2^{n-i} - 23)$.

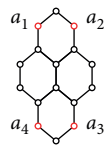

$w_v(a_j) = 19 \times 2^n - 18$, $s_v(a_j) = 23 \times 2^n - 23$, $j = 1, 2, 3, 4$

FIGURE 3: Quotient graph Gn/E_1.

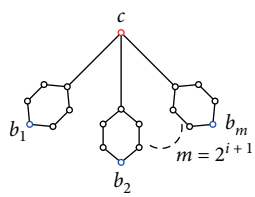

$w_v(b_k) = 19 \times 2^{n-i+1} - 24$, $s_v(b_k) = 23 \times 2^{n-i+1} - 30$, $k = 1, 2, ..., m$
$w_v(c) = 38 \times 2^i - 60$, $s_v(c) = 46 \times 2^i - 73$

FIGURE 4: Quotient graph $Gn/E_{2i} : 1 \le i \le n$.

For the remaining vertices, vertex weight is 1 and vertex strength is 0.

Consider the quotient graph Gn/E_1 (Figure 3). Using transmission index method [68], the Wiener index for a graph G is defined as, $W(G) = \frac{T(p)}{2}$, where $p \in V(G)$ and $T(p)$ is the transmission index of vertex p.

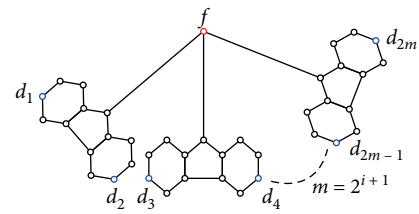

$w_v(d_r) = 19 \times 2^{n-i} - 18$, $s_v(d_r) = 23 \times 2^{n-i} - 23$, $r = 1, 2, ..., 2m$
$w_v(f) = 50 \times 2^i - 60$, $s_v(f) = 60 \times 2^i - 73$

FIGURE 5: Quotient graph $Gn/E_{2i+1} : 1 \le i \le n$.

$$\begin{aligned}
\text{Therefore, } W(Gn/E_1) &= \frac{T(p)}{2}, p \in V(Gn/E_1) \\
&= 24w_v(a_j)^2 + 152w_v(a_j) + 186, \\
&\quad \text{where } (w_v(a_j), s_v(a_j)) \\
&= (19 \times 2^n - 18, 23 \times 2^n - 23). \\
\text{Hence, } W(Gn/E_1) &= 2{,}888 \times 2^n + 24(19 \times 2^n - 18)^2 - 2{,}550.
\end{aligned} \tag{7}$$

$$\begin{aligned}
\text{Also, } Sz_v(Gn/E_1) &= 12(4 + w_v(a_j))(8 + 3w_v(a_j)) + 4(1 + 2w_v(a_j))(11 + 2w_v(a_j)) \\
&\quad + 3(6 + 2w_v(a_j))(6 + 2w_v(a_j)), \\
&= 23{,}104 \times 2^{2n} - 36{,}024 \times 2^n + 13{,}928. \\
Sz_e(Gn/E_1) &= 12(s_v(a_j) + 4)(3s_v(a_j) + 12) + 4(2 + 2s_v(a_j))(15 + 2s_v(a_j)) \\
&\quad + 3(8 + 2s_v(a_j))(8 + 2s_v(a_j)), \\
&= 33{,}856 \times 2^{2n} - 55{,}752 \times 2^n + 22{,}784. \\
\mathrm{PI}(Gn/E_1) &= 12((s_v(a_j) + 4) + (3s_v(a_j) + 12)) + 4((2 + 2s_v(a_j)) + (15 + 2s_v(a_j)) \\
&\quad + 3((8 + 2s_v(a_j) + (8 + 2s_v(a_j))), \\
&= 1{,}748 \times 2^n - 1{,}440.
\end{aligned} \tag{8}$$

$$\begin{aligned}
\mathrm{Mo}(Gn/E_1) &= 12|(4 + w_v(a_j)) - (8 + 3w_v(a_j))| + 4|(1 + 2w_v(a_j)) - (11 + 2w_v(a_j))| \\
&\quad + 3|(6 + 2w_v(a_j)) - (6 + 2w_v(a_j)), \\
&= 456 \times 2^n - 344. \\
\mathrm{Mo}_e(Gn/E_1) &= 12|(s_v(a_j) + 4) - (3s_v(a_j) + 12)| + 4|(2 + 2s_v(a_j)) - (15 + 2s_v(a_j))| \\
&\quad + 3|((8 + 2s_v(a_j)) - (8 + 2s_v(a_j))|, \\
&= 552 \times 2^n - 404.
\end{aligned} \tag{9}$$

Consider Gn/E_{2i} (Figure 4), with $w_v(c) = 38 \times 2^i - 60$, $s_v(c) = 46 \times 2^i - 73$, $w_v(b_k) = 19 \times 2^{n-i+1} - 24$, $s_v(b_k) = 23 \times 2^{n-i+1} - 30$ and $m = 2^{i+1} : 1 \le i \le n$.

Using Theorem 1:

$$\begin{aligned} W(Gn/E_{2i}) &= 18m + 9mw_v(b_k) + 11mw_v(c) + 4mw_v(b_k)w_v(c) + 4m(m-1)(w_v(b_k))^2 \\ &\quad + 31m(m-1)w_v(b_k) + 55m(m-1), \\ &= 38(173\times 2^i - 304\times 2^{2n-i} - 340\times 2^{i+n} + 608\times 2^{2n} - 140\times 2^n). \\ \text{Hence, } \sum_{i=1}^{n} W(Gn/E_{2i}) &= 50{,}540\times 2^n - 37{,}392\times 2^{2n} + n(23{,}104\times 2^{2n} - 5{,}320\times 2^n) - 13{,}148. \end{aligned} \tag{10}$$

$$\begin{aligned} \text{Also, } Sz_v(Gn/E_{2i}) &= 2^{i+1}(5 + w_v(b_k))(5(m-1) + w_v(b_k)(m-1) + w_v(c)) \\ &\quad + 6\times 2^{i+1}(2 + w_v(b_k))(5(m-1) + w_v(b_k)(m-1) + w_v(c) + 3), \\ &= 38(305\times 2^i - 532\times 2^{2n-i} - 604\times 2^{i+n} + 1{,}064\times 2^{2n} - 236\times 2^n). \\ \sum_{i=1}^{n} Sz_v(Gn/E_{2i}) &= 89{,}300\times 2^n - 66{,}120\times 2^{2n} - 8{,}968n\times 2^n + 40{,}432n\times 2^{2n} - 23{,}180. \end{aligned} \tag{11}$$

$$\begin{aligned} Sz_e(Gn/E_{2i}) &= 2^{i+1}(6 + s_v(b_k))(7(m-1) + s_v(b_k)(m-1) + s_v(c)) \\ &\quad + 6\times 2^{i+1}(2 + s_v(b_k))(7(m-1) + s_v(b_k)(m-1) + s_v(c) + 3), \\ &= 8(2{,}274\times 2^i - 3{,}703\times 2^{2n-i} - 4{,}416\times 2^{i+n} + 7{,}406\times 2^{2n} - 1{,}610\times 2^n). \\ \sum_{i=1}^{n} Sz_e(Gn/E_{2i}) &= 136{,}664\times 2^n - 100{,}280\times 2^{2n} - 12{,}880n\times 2^n + 59{,}248n\times 2^{2n} - 36{,}384. \end{aligned} \tag{12}$$

$$\begin{aligned} \mathrm{PI}(Gn/E_{2i}) &= 2^{i+1}[(6 + s_v(b_k)) + (7(m-1) + s_v(b_k)(m-1) + s_v(c))] \\ &\quad + 6\times 2^{i+1}[(2 + s_v(b_k)) + (7(m-1) + s_v(b_k)(m-1) + s_v(c) + 3)], \\ &= 8\times 2^i(161\times 2^n - 131). \\ \sum_{i=1}^{n} \mathrm{PI}(Gn/E_{2i}) &= 2{,}576\times 2^{2n} - 4{,}672\times 2^n + 2{,}096. \end{aligned} \tag{13}$$

$$\begin{aligned} \mathrm{Mo}(Gn/E_{2i}) &= 2^{i+1}|(5 + w_v(b_k)) - (5(m-1) + w_v(b_k)(m-1) + w_v(c))| \\ &\quad + 6\times 2^{i+1}|(2 + w_v(b_k)) - (5(m-1) + w_v(b_k)(m-1) + w_v(c) + 3)|, \\ &= 1{,}064\times 2^{n+i} - 1{,}064\times 2^n - 236\times 2^i. \\ \sum_{i=1}^{n} \mathrm{Mo}(Gn/E_{2i}) &= 2{,}128\times 2^{2n} - 1{,}064n\times 2^n - 2{,}600\times 2^n + 472. \end{aligned} \tag{14}$$

$$\begin{aligned} \mathrm{Mo}_e(Gn/E_{2i}) &= 2^{i+1}|(6 + s_v(b_k)) - (7(m-1) + s_v(b_k)(m-1) + s_v(c))| \\ &\quad + 6\times 2^{i+1}|(2 + s_v(b_k)) - (7(m-1) + s_v(b_k)(m-1) + s_v(c) + 3)|, \\ &= 1{,}288\times 2^{n+i} - 1{,}288\times 2^n - 280\times 2^i. \\ \sum_{i=1}^{n} \mathrm{Mo}_e(Gn/E_{2i}) &= 2{,}576\times 2^{2n} - 1{,}288n\times 2^n - 3{,}136\times 2^n + 560. \end{aligned} \tag{15}$$

Consider Gn/E_{2i+1} (Figure 5). Computing the indices likewise in quotient graph Gn/E_{2i}, we obtain the following equations.

$W(Gn/E_{2i+1}) = 2(5{,}649\times 2^i - 5{,}415\times 2^{2n-i} - 11{,}172\times 2^{i+n} + 14{,}440\times 2^{2n+i} - 3{,}154\times 2^n)$,

$\sum_{i=1}^{n} W(Gn/E_{2i+1}) = 78{,}114\times 2^n - 55{,}518\times 2^{2n} + n(28{,}880\times 2^{2n} - 6{,}308\times 2^n) - 22{,}596$,

$Sz_v(Gn/E_{2i+1}) = 2(11{,}450\times 2^i - 11{,}191\times 2^{2n-i} - 23{,}332\times 2^{i+n} + 28{,}880\times 2^{2n} - 5{,}168\times 2^n)$,

$\sum_{i=1}^{n} Sz_v(Gn/E_{2i+1}) = 161{,}510 \times 2^n - 10{,}336n \times 2^n - 115{,}710 \times 2^{2n} + 57{,}760n \times 2^{2n} - 45{,}800$,

$Sz_e(Gn/E_{2i+1}) = 2(17{,}773 \times 2^i - 16{,}399 \times 2^{2n-i} - 35{,}604 \times 2^{i+n} + 42{,}320 \times 2^{2n} - 7{,}406 \times 2^n)$,

$\sum_{i=1}^{n} Sz_e(Gn/E_{2i+1}) = 246{,}306 \times 2^n - 14{,}812n \times 2^n - 175{,}214 \times 2^{2n} + 84{,}640n \times 2^{2n} - 71{,}092$,

$\mathrm{PI}(Gn/E_{2i+1}) = 40 \times 2^i(69 \times 2^n - 56)$,

$\sum_{i=1}^{n} \mathrm{PI}(Gn/E_{2i+1}) = 5{,}520 \times 2^{2n} - 10{,}000 \times 2^n + 4{,}480$,

$\mathrm{Mo}(Gn/E_{2i+1}) = 2{,}280 \times 2^{n+i} - 1{,}596 \times 2^n - 532 \times 2^i$,

$\sum_{i=1}^{n} \mathrm{Mo}(Gn/E_{2i+1}) = 4{,}560 \times 2^{2n} - 1{,}596n \times 2^n - 5{,}624 \times 2^n + 1{,}064$,

$\mathrm{Mo}_e(Gn/E_{2i+1}) = 2{,}760 \times 2^{n+i} - 1{,}932 \times 2^n - 628 \times 2^i$,

$\sum_{i=1}^{n} \mathrm{Mo}_e(Gn/E_{2i+1}) = 5{,}520 \times 2^{2n} - 1{,}932n \times 2^n - 6{,}776 \times 2^n + 1{,}256$.

Using Theorem 1 [34], we get the following equations:

$$\begin{aligned} W(Gn) &= W(Gn/E_1) + \sum_{i=1}^{n} W(Gn/E_{2i}) + \sum_{i=1}^{n} W(Gn/E_{2i+1}), \\ &= (115{,}126 - 11{,}628n) \times 2^n + (51{,}984n - 84{,}246) \times 2^{2n} - 30{,}518. \\ Sz_v(Gn) &= Sz_v(Gn/E_1) + \sum_{i=1}^{n} Sz_v(Gn/E_{2i}) + \sum_{i=1}^{n} Sz_v(Gn/E_{2i+1}), \\ &= (214{,}786 - 19{,}304n) \times 2^n + (98{,}192n - 158{,}726) \times 2^{2n} - 55{,}052. \end{aligned} \tag{16}$$

$$\begin{aligned} Sz_e(Gn) &= Sz_e(Gn/E_1) + \sum_{i=1}^{n} Sz_e(Gn/E_{2i}) + \sum_{i=1}^{n} Sz_e(Gn/E_{2i+1}), \\ &= (327{,}218 - 27{,}692n) \times 2^n + (143{,}888n - 241{,}638) \times 2^{2n} - 84{,}692. \\ \mathrm{PI}(Gn) &= \mathrm{PI}(Gn/E_1) + \sum_{i=1}^{n} \mathrm{PI}(Gn/E_{2i}) + \sum_{i=1}^{n} \mathrm{PI}(Gn/E_{2i+1}), \\ &= 8{,}096 \times 2^{2n} - 12{,}924 \times 2^n + 5{,}136. \\ \mathrm{Mo}(Gn) &= \mathrm{Mo}(Gn/E_1) + \sum_{i=1}^{n} \mathrm{Mo}(Gn/E_{2i}) + \sum_{i=1}^{n} \mathrm{Mo}(Gn/E_{2i+1}), \\ &= 6{,}688 \times 2^{2n} - (2{,}660n + 7{,}768) \times 2^n + 1{,}192. \\ \mathrm{Mo}_e(Gn) &= \mathrm{Mo}_e(Gn/E_1) + \sum_{i=1}^{n} \mathrm{Mo}_e(Gn/E_{2i}), + \sum_{i=1}^{n} \mathrm{Mo}_e(Gn/E_{2i+1}) \\ &= 8{,}096 \times 2^{2n} - (3{,}220n + 9{,}360) \times 2^n + 1{,}412. \end{aligned} \tag{17}$$

□

Theorem 3. *For $n \geq 0$:*

$W(PyGn) = (720n + 10{,}996) \times 2^n + (14{,}400n - 2{,}340) \times 2^{2n} - 430$,

$Sz_v(PyGn) = (1{,}080n + 14{,}428) \times 2^n + (21{,}600n + 2{,}280) \times 2^{2n} - 476$,

$Sz_e(PyGn) = (2{,}040n + 21{,}032) \times 2^n + (27{,}744n - 3{,}400) \times 2^{2n} - 492$,

$\mathrm{PI}(PyGn) = 4{,}624 \times 2^{2n} - 1{,}884 \times 2^n + 172$,

$\mathrm{Mo}(PyGn) = 4{,}080 \times 2^{2n} - (720n + 2{,}272) \times 2^n - 96$,

$\mathrm{Mo}_e(PyGn) = 4{,}624 \times 2^{2n} - (816n + 2{,}464) \times 2^n - 140$.

Proof. The graph $PyGn$ has $60 \times 2^n - 12$ vertices, $68 \times 2^n - 13$ edges, and $44 \times 2^n - 13$ Θ^*-classes. Let us consider $PyG2$. The sets E_i, which is coarser than the Θ^*-classes chosen for $PyG2$ are highlighted in Figure 6. We convert the original graph into quotient graphs and we obtain $(n+2)$ quotient graphs for $PyGn$. There are three types of weighted quotient graphs $\{PyGn/E_1, PyGn/E_i, PyGn/E_{n+2} : 2 \leq i \leq n+1, n \geq 0\}$ for $PyGn$.

The first type of quotient graph $PyGn/E_1$ has 16 vertices and 19 edges, among which four vertices, $a_j : 1 \leq j \leq 4$ has $(w_v(a_j), s_v(a_j)) = (15 \times 2^n - 6, 17 \times 2^n - 8)$ and for remaining vertices, vertex weight is 1 and vertex strength is 0, as given in Figure 7.

The second type of quotient graph $PyGn/E_i : 2 \leq i \leq n+1$ has a weighted core vertex, say c attached with $m = 2^i : 2 \leq i \leq n+1$ branches such that two vertices in each branch has same weighted values, as given in Figure 8. Let us take those vertices to be $b_k : 1 \leq k \leq 2m$. Then, $(w_v(c), s_v(c)) = (7 \times 2^i - 12, 8 \times 2^i - 13)$,

$(w_v(b_k), s_v(b_k)) = (15 \times 2^{n-i+1} - 6, 17 \times 2^{n-i+1} - 8)$.

For the remaining vertices, vertex weight and vertex strength is 1 and 0, respectively.

The third type of quotient graph $PyGn/E_{n+2}$ has a weighted core vertex, say d attached with $m = 2^{n+2}$ branches, as given in Figure 9, where $(w_v(d), s_v(d)) = (28 \times 2^n - 12, 32 \times 2^n - 13)$ and all other vertices have vertex weight and vertex strength equal to 1 and 0, respectively.

Proceeding with the similar pattern applied in computing the indices of quotient graphs for Gn, we obtain the following for $PyGn$.

For $PyGn/E_1$ (Figure 7):

$W(PyGn/E_1) = 2{,}280 \times 2^n + 24(15 \times 2^n - 6)^2 - 726$,

$Sz_v(PyGn/E_1) = 14{,}400 \times 2^{2n} - 5{,}400 \times 2^n + 392$,

$Sz_e(PyGn/E_1) = 18{,}496 \times 2^{2n} - 8{,}568 \times 2^n + 824$;

$\mathrm{PI}(PyGn/E_1) = 1{,}292 \times 2^n - 300$,

$\mathrm{Mo}(PyGn/E_1) = 360 \times 2^n - 56$; $\mathrm{Mo}_e(PyGn/E_1) = 408 \times 2^n - 44$.

For $PyGn/E_i$ (Figure 8):

$W(PyGn/E_i) = 2(71 \times 2^i - 6{,}300 \times 2^{2n-i} - 1{,}020 \times 2^{i+n} + 7{,}200 \times 2^{2n} + 360 \times 2^n)$,

$\sum_{i=2}^{n+1} W(PyGn/E_i) = 15{,}028 \times 2^n - 14{,}460 \times 2^{2n} + n(14{,}400 \times 2^{2n} + 720 \times 2^n) - 568$,

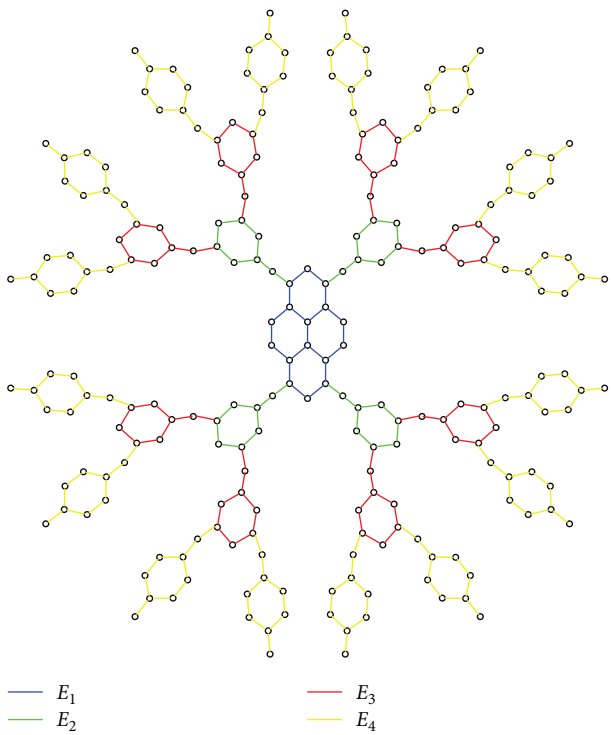

FIGURE 6: Illustration of sets E_i of $PyG2$.

$Sz_v(PyGn/E_i) = 217 \times 2^i - 18{,}000 \times 2^{2n-i} - 3{,}180 \times 2^{i+n} + 21{,}600 \times 2^{2n} + 1{,}080 \times 2^n$,

$\sum_{i=2}^{n+1} Sz_v(PyGn/E_i) = 22{,}588 \times 2^n - 21{,}720 \times 2^{2n} + n(21{,}600 \times 2^{2n} + 1{,}080 \times 2^n) - 868$,

$Sz_e(PyGn/E_i) = 329 \times 2^i - 23{,}120 \times 2^{2n-i} - 4{,}828 \times 2^{i+n} + 27{,}744 \times 2^{2n} + 2{,}040 \times 2^n$,

$\sum_{i=2}^{n+1} Sz_e(PyGn/E_i) = 2{,}040n \times 2^n - 30{,}872 \times 2^{2n} + 32{,}188 \times 2^n + 27{,}744n \times 2^{2n} - 1{,}316$,

$\mathrm{PI}(PyGn/E_i) = 2^{i+1}(272 \times 2^n - 59)$,

$\sum_{i=2}^{n+1} \mathrm{PI}(PyGn/E_i) = 2{,}176 \times 2^{2n} - 2{,}648 \times 2^n + 472$,

$\mathrm{Mo}(PyGn/E_i) = 10 \times 2^i - 720 \times 2^n + 480 \times 2^{n+i}$,

$\sum_{i=2}^{n+1} \mathrm{Mo}(PyGn/E_i) = 1{,}920 \times 2^{2n} - 720n \times 2^n - 1{,}880 \times 2^n - 40$,

$\mathrm{Mo}_e(PyGn/E_i) = 24 \times 2^i - 816 \times 2^n + 544 \times 2^{n+i}$,

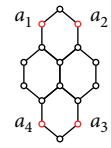

$w_v(a_j) = 15 \times 2^n - 6$, $s_v(a_j) = 17 \times 2^n - 8$, $j = 1, 2, 3, 4$

FIGURE 7: Quotient graph $PyGn/E_1$.

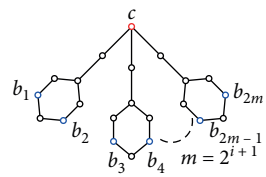

$w_v(b_k) = 15 \times 2^{n-i+1} - 6$, $s_v(b_k) = 17 \times 2^{n-i+1} - 8$, $k = 1, 2, \ldots, 2m$
$w_v(c) = 7 \times 2^i - 12$, $s_v(c) = 8 \times 2^i - 13$

FIGURE 8: Quotient graph $PyGn/E_i : 1 \le i \le n+1$.

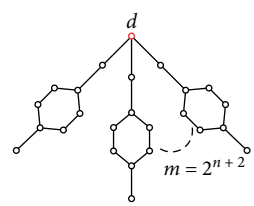

$w_v(d) = 28 \times 2^n - 12$, $s_v(d) = 32 \times 2^n - 13$

FIGURE 9: Quotient graph $PyGn/E_{n+2}$.

$\sum_{i=2}^{n+1} \mathrm{Mo}_e(PyGn/E_i) = 2{,}176 \times 2^{2n} - 816n \times 2^n - 2{,}080 \times 2^n - 96$.

For $PyGn/E_{n+2}$ (Figure 9):

$W(PyGn/E_{n+2}) = 24 \times 2^n(280 \times 2^n - 83)$;

$Sz_v(PyGn/E_{n+2}) = 120 \times 2^n(80 \times 2^n - 23)$,

$Sz_e(PyGn/E_{n+2}) = 4 \times 2^n(2{,}244 \times 2^n - 647)$;

$\mathrm{PI}(PyGn/E_{n+2}) = 48 \times 2^n(51 \times 2^n - 11)$,

$\mathrm{Mo}(PyGn/E_{n+2}) = 16 \times 2^n(135 \times 2^n - 47)$;

$\mathrm{Mo}_e(PyGn/E_{n+2}) = 72 \times 2^n(34 \times 2^n - 11)$.

By Theorem 1 [34], we get the following equations:

$$\begin{aligned}
W(PyGn) &= W(PyGn/E_1) + \sum_{i=2}^{n+1} W(PyGn/E_i) + W(PyGn/E_{n+2}), \\
&= (720n + 10{,}996) \times 2^n + (14{,}400n - 2{,}340) \times 2^{2n} - 430. \\
Sz_v(PyGn) &= Sz_v(PyGn/E_1) + \sum_{i=2}^{n+1} Sz_v(PyGn/E_i) + Sz_v(PyGn/E_{n+2}), \\
&= (1{,}080n + 14{,}428) \times 2^n + (21{,}600n + 2{,}280) \times 2^{2n} - 476. \\
Sz_e(PyGn) &= Sz_e(PyGn/E_1) + \sum_{i=2}^{n+1} Sz_e(PyGn/E_i) + Sz_e(PyGn/E_{n+2}), \\
&= (2{,}040n + 21{,}032) \times 2^n + (27{,}744n - 3{,}400) \times 2^{2n} - 492. \\
\mathrm{PI}(PyGn) &= \mathrm{PI}(PyGn/E_1) + \sum_{i=2}^{n+1} \mathrm{PI}(PyGn/E_i) + \mathrm{PI}(PyGn/E_{n+2}), \\
&= 4{,}624 \times 2^{2n} - 1{,}884 \times 2^n + 172.
\end{aligned} \tag{18}$$

$$\begin{aligned}\mathrm{Mo}(PyGn) &= \mathrm{Mo}(PyGn/E_1) + \sum_{i=2}^{n+1}\mathrm{Mo}(PyGn/E_i) + \mathrm{Mo}(PyGn/E_{n+2}),\\ &= 4{,}080\times 2^{2n} - (720n + 2{,}272)\times 2^n - 96.\\ \mathrm{Mo}_e(PyGn) &= \mathrm{Mo}_e(PyGn/E_1) + \sum_{i=2}^{n+1}\mathrm{Mo}_e(PyGn/E_i) + \mathrm{Mo}_e(PyGn/E_{n+2}),\\ &= 4{,}624\times 2^{2n} - (816n + 2{,}464)\times 2^n - 140.\end{aligned} \tag{19}$$

□

4. Degree-Based Index and Graph Entropy

In this section, we compute the degree-based indices defined in Table 1 for the pyrene cored dendrimers Gn and $PyGn$. Further, we have extended the work to the degree-based entropy measures of the dendrimers. We have used degree counting method and edge partition based on the vertices and edges of the dendrimer structure to compute the degree-based indices and further the graph entropies were determined using Equation (5) given in Section 2.

4.1. Theorems on Degree-Based Index and Entropy of Gn

Theorem 4. *For $n \geq 1$:*

$M_1(Gn) = 464\times 2^n - 370$,
$M_2(Gn) = 588\times 2^n - 467$,
$H(Gn) = \frac{1}{3}(112\times 2^n - 88)$,
$HM(Gn) = 2{,}392\times 2^n - 1{,}908$,
$F(Gn) = 1{,}216\times 2^n - 974$,
$R(Gn) = \frac{\sqrt{6}}{6}(40\times 2^n - 40) + \frac{1}{3}(64\times 2^n - 40)$,
$RR(Gn) = \sqrt{6}(40\times 2^n - 40) + 132\times 2^n - 85$,
$SC(Gn) = \frac{\sqrt{6}}{6}(28\times 2^n - 19) + \frac{\sqrt{5}}{5}(40\times 2^n - 40) + 12\times 2^n - 7$,
$GA(Gn) = \frac{2\sqrt{6}}{5}(40\times 2^n - 40) + 52\times 2^n - 33$,
$ABC(Gn) = 32\sqrt{2}\times 2^n - 27\sqrt{2} + \frac{1}{3}(56\times 2^n - 38)$, *and*
$irr(Gn) = \sigma(Gn) = 40\times 2^n - 40$.

Proof. The graph $Gn : n \geq 1$ has $92\times 2^n - 73$ edges. The degree of vertices of Gn is either 2 or 3 and by observation, we inferred three partitions for the edge set based on the vertex degree, which are $(2,2)$, $(2,3)$, and $(3,3)$. The edge partitions $(d_p, d_q), pq \in E(Gn)$ and the corresponding number of edges in each partition is given in Table 3. The second-generation pyrene cored dendrimer $G2$ is given in Figure 1.

Using Table 3 and by applying formulas in Table 1, we derive the following equation:

$$\begin{aligned}M_1(Gn) &= 4(24\times 2^n - 14) + 5(40\times 2^n - 40) + 6(28\times 2^n - 19),\\ &= 464\times 2^n - 370.\\ M_2(Gn) &= 4(24\times 2^n - 14) + 6(40\times 2^n - 40) + 9(28\times 2^n - 19),\\ &= 588\times 2^n - 467.\\ H(Gn) &= \frac{1}{2}(24\times 2^n - 14) + \frac{2}{5}(40\times 2^n - 40) + \frac{1}{3}(28\times 2^n - 19),\\ &= \frac{1}{3}(112\times 2^n - 88).\end{aligned} \tag{20}$$

Proceeding likewise, the remaining degree-based indices are obtained. □

Theorem 5. *For $n \geq 1$:*

$$\mathrm{ENT}_{M_1}(Gn) = \log(464\times 2^n - 370) - \frac{425583089622851948\times 2^n - 339898286655842223}{1125899906842624(232\times 2^n - 185)}, \tag{21}$$

$$\mathrm{ENT}M_2(Gn) = \log(588\times 2^n - 467) - \frac{628706518870406948\times 2^n - 497298819678705633}{562949953421312(588\times 2^n - 467)}, \tag{22}$$

$$\mathrm{ENT}_H(Gn) = \log\left(\frac{1}{3}(112\times 2^n - 88)\right) + \frac{448992659589657384\times 2^n - 357638409783584073}{36028797018963968(14\times 2^n - 11)}, \tag{23}$$

Table 3: Edge partition of the pyrene cored dendrimer G_n.

Edge partition (d_p, d_q)	(2,2)	(2,3)	(3,3)
Number of edges	$24\times 2^n - 14$	$40\times 2^n - 40$	$28\times 2^n - 19$

$$\mathrm{ENT}_{HM}(Gn) = \log(2{,}392\times 2^n - 1{,}908) - \frac{555613095933322220\times 2^n - 442694178403221039}{281474976710656(598\times 2^n - 477)}, \tag{24}$$

$$\mathrm{ENT}_{F}(Gn) = \log(1{,}216\times 2^n - 974) - \frac{224460377070067932\times 2^n - 179804685288579973}{140737488355328(608\times 2^n - 487)}, \tag{25}$$

$$\mathrm{ENT}_{R}(Gn) = \log\left(\frac{\sqrt{6}}{6}(40\times 2^n - 40) + \frac{1}{3}(64\times 2^n - 40)\right) + \frac{\left(\frac{74762311106051279\times 2^n}{2251799813685248}\right) - \left(\frac{119073205610078121}{4503599627370496}\right)}{\frac{\sqrt{6}}{6}(40\times 2^n - 40) + \frac{1}{3}(64\times 2^n - 40)}, \tag{26}$$

$$\mathrm{ENT}_{RR}(Gn) = \log\left(\sqrt{6}(40\times 2^n - 40) + 132\times 2^n - 85\right) - \frac{\left(\frac{150119348919218 85\times 2^n}{70368744177664}\right) - \left(\frac{191185629566711927}{1125899906842624}\right)}{\sqrt{6}(40\times 2^n - 40) + 132\times 2^n - 85}, \tag{27}$$

$$\begin{aligned}\mathrm{ENT}_{SC}(Gn) = {} & \log\left(\frac{\sqrt{6}}{6}(28\times 2^n - 19) + \frac{\sqrt{5}}{5}(40\times 2^n - 40) + 12\times 2^n - 7\right) \\ & + \frac{\left(\frac{148410608094732093\times 2^n}{4503599627370496}\right) - \left(\frac{471911787562986329}{18014398509481984}\right)}{\left(\frac{\sqrt{6}}{6}(28\times 2^n - 19) + \frac{\sqrt{5}}{5}(40\times 2^n - 40) + 12\times 2^n - 7\right.},\end{aligned} \tag{28}$$

$$\mathrm{ENT}_{GA}(Gn) = \log\left(\frac{2\sqrt{6}}{5}(40\times 2^n - 40) + 52\times 2^n - 33\right) + \frac{\left(\frac{1801314774408985\times 2^n}{2251799813685248}\right) - \left(\frac{1801314774408985}{2251799813685248}\right)}{\frac{2\sqrt{6}}{5}(40\times 2^n - 40) + 52\times 2^n - 33}, \tag{29}$$

$$\mathrm{ENT}_{ABC}(Gn) = \log\left(32\sqrt{2}\times 2^n - 27\sqrt{2} + \frac{1}{3}(56\times 2^n - 38)\right) - \frac{3\times\left\{\left(\frac{1047213568704659 57\times 2^n}{4503599627370496}\right) - \left(\frac{330913265150441377}{18014398509481984}\right)\right\}}{81\sqrt{2} - 96\sqrt{2}\times 2^n - 56\times 2^n + 38}. \tag{30}$$

$$\mathrm{ENT}_{irr}(Gn) = \mathrm{ENT}_{\sigma}(Gn) = \log(40\times 2^n - 40).$$

Proof. Using Equation (5):

$$\mathrm{ENT}_{M_1}(Gn) = \log(M_1(Gn)) - \frac{1}{M_1(Gn)}\sum_{pq\in E(Gn)}(d_p + d_q)\log(d_p + d_q). \tag{31}$$

Therefore, using data from Theorem 4:

$$\begin{aligned}\mathrm{ENT}_{M_1}(Gn) &= \log(464\times 2^n - 370) - \frac{1}{(464\times 2^n - 370)}\{4\log(4)(24\times 2^n - 14) \\ &\quad + 5\log(5)(40\times 2^n - 40) + 6\log(6)(28\times 2^n - 19)\}, \\ &= \log(464\times 2^n - 370) - \frac{425583089622851948\times 2^n - 339898286655842223}{1125899906842624(232\times 2^n - 185)}.\end{aligned} \tag{32}$$

Table 4: Edge partition of the pyrene cored dendrimer *PyGn*.

Edge partition (d_p, d_q)	(1,3)	(2,2)	(2,3)	(3,3)
Number of edges	4×2^n	$8\times 2^n+2$	$56\times 2^n-24$	9

Proceeding in the similar manner:

$$\begin{aligned}\mathrm{ENT}_{M_2}(Gn) &= \log(M_2(Gn)) - \frac{1}{M_2(Gn)}\sum_{pq\in E(Gn)}\left(d_p\times d_q\right)\log\left(d_p\times d_q\right),\\ &= \log(588\times 2^n-467) - \frac{628706518870406948\times 2^n - 497298819678705633}{562949953421312(588\times 2^n-467)}.\end{aligned} \tag{33}$$

Proceeding further in the similar way, the remaining entropy mesaures are obtained. □

4.2. Theorems on Degree-Based Index and Entropy of PyGn

Theorem 6. *For $n\geq 0$:*

$M_1(PyGn) = 328\times 2^n - 58,$
$M_2(PyGn) = 380\times 2^n - 55,$
$H(PyGn) = \frac{1}{5}(142\times 2^n - 28),$
$HM(PyGn) = 1{,}592\times 2^n - 244,$
$F(PyGn) = 832\times 2^n - 134,$
$R(PyGn) = \frac{\sqrt{6}}{6}(56\times 2^n - 24)) + \frac{1}{3}(4\sqrt{3}\times 2^n) + 4\times 2^n + 4,$
$RR(PyGn) = \sqrt{6}(56\times 2^n - 24) + 4\sqrt{3}\times 2^n + 16\times 2^n + 31,$
$SC(PyGn) = \frac{3\sqrt{6}}{2} + \frac{\sqrt{5}}{5}(56\times 2^n - 24) + 6\times 2^n + 1,$
$GA(PyGn) = \frac{2\sqrt{6}}{5}(56\times 2^n - 24) + 2\sqrt{3}\times 2^n + 8\times 2^n + 11,$
$ABC(PyGn) = 32\sqrt{2}\times 2^n - 11\sqrt{2} + \frac{1}{3}(4\sqrt{6}\times 2^n) + 6,$
$irr(PyGn) = 64\times 2^n - 24,$
$\sigma(PyGn) = 72\times 2^n - 24.$

Proof. The graph $PyGn : n\geq 0$ has $68\times 2^n - 13$ edges with four edge partitions, say $(1,3)$, $(2,2)$, $(2,3)$, and $(3,3)$. The number of edges in each partition is given in Table 4.

The remaining proof is similar to Theorem 4. □

Theorem 7. *For $n\geq 0$:*

$$\mathrm{ENT}_{M_1}(PyGn) = \log(328\times 2^n - 58) - \frac{291149128003987866\times 2^n - 48012415846364161}{1125899906842624(164\times 2^n - 29)}, \tag{34}$$

$$\mathrm{ENT}_{M_2}(PyGn) = \log(380\times 2^n - 55) - \frac{371308249587494075\times 2^n - 38814170884114593}{2814749767106560(76\times 2^n - 11)}, \tag{35}$$

$$\mathrm{ENT}_{H}(PyGn) = \log\left(\frac{142}{5}\times 2^n - \frac{28}{5}\right) + \frac{1111659321138413130\times 2^n - 216506362811685245}{18014398509481984(71\times 2^n - 14)}, \tag{36}$$

$$\mathrm{ENT}_{HM}(PyGn) = \log(1592\times 2^n - 244) - \frac{(354571437852736794\times 2^n - 47959291218450817)}{281474976710656(398\times 2^n - 61)}, \tag{37}$$

$$\mathrm{ENT}_{F}(PyGn) = \log(832\times 2^n - 134) - \frac{294489084091593460\times 2^n - 42045734203777869}{281474976710656(416\times 2^n - 67)}, \tag{38}$$

Table 5: Computed numerical values of indices for initial generations of dendrimer Gn.

Topological index	$n=1$	$n=2$	$n=3$	$n=4$	$n=5$	$n=6$
Wiener	47,430	652,514	5,200,602	32,731,946	181,683,210	935,359,562
Szeged	93,776	1,252,188	9,894,340	62,060,820	343,937,076	1,769,303,412
Edge Szeged	123,360	1,740,852	14,030,108	88,860,492	495,224,812	2,556,665,772
Padmakar–Ivan	11,672	82,976	419,888	1,870,928	7,881,872	32,339,216
Mostar	7,088	55,848	303,240	1,418,792	6,175,528	25,876,648
Edge Mostar	8,636	67,748	367,396	1,718,148	7,476,996	31,327,108

$$\mathrm{ENT}_R(PyGn) = \log\left(\frac{\sqrt{6}}{6}(56\times 2^n - 24) + \frac{4\sqrt{3}}{3}\times 2^n + 4\times 2^n + 4\right) + \frac{\left(\frac{110440303912309195\times 2^n}{4503599627370496}\right) - \left(\frac{43133755380997165}{9007199254740992}\right)}{\frac{\sqrt{6}}{6}(56\times 2^n - 24) + \frac{4\sqrt{3}}{3}\times 2^n + 4\times 2^n + 4}, \quad (39)$$

$$\mathrm{ENT}_{RR}(PyGn) = \log\left(\sqrt{6}(56\times 2^n - 24) + 4\sqrt{3}\times 2^n + 16\times 2^n + 31\right) - \frac{\left(\frac{77566149320825541\times 2^n}{562949953421312}\right) - \left(\frac{45557595933161857}{2251799813685248}\right)}{\sqrt{6}(56\times 2^n - 24) + 4\sqrt{3}\times 2^n + 16\times 2^n + 31}, \quad (40)$$

$$\mathrm{ENT}_{SC}(PyGn) = \log\left(\frac{3\sqrt{6}}{2} + \frac{\sqrt{5}}{5}(56\times 2^n - 24) + 6\times 2^n + 1\right) + \frac{\left(\frac{109492565816084565\times 2^n}{4503599627370496}\right) - \left(\frac{41904469388909117}{9007199254740992}\right)}{\frac{3\sqrt{6}}{2} + \frac{\sqrt{5}}{5}(56\times 2^n - 24) + 6\times 2^n + 1}, \quad (41)$$

$$\mathrm{ENT}_{GA}(PyGn) = \log\left(\frac{2\sqrt{6}}{5}(56\times 2^n - 24) + 2\sqrt{3}\times 2^n + 8\times 2^n + 11\right) + \frac{\left(\frac{29150939348632037\times 2^n}{18014398509481984}\right) - \left(\frac{1080788864645391}{2251799813685248}\right)}{\frac{2\sqrt{6}}{5}(56\times 2^n - 24) + 2\sqrt{3}\times 2^n + 8\times 2^n + 11}, \quad (42)$$

$$\mathrm{ENT}_{ABC}(PyGn) = \log\left(32\sqrt{2}\times 2^n - 11\sqrt{2} + \frac{4\sqrt{6}}{3}\times 2^n + 6\right) + \frac{3\times\left\{\left(\frac{147233949232203497\times 2^n}{9007199254740992}\right) - \left(\frac{3331120273589785}{1125899906842624}\right)\right\}}{96\sqrt{2}\times 2^n - 33\sqrt{2} + 4\sqrt{6}\times 2^n + 18}, \quad (43)$$

$$\mathrm{ENT}_{irr}(PyGn) = \log(64\times 2^n - 24) - \frac{(6243314768165359\times 2^n)}{1125899906842624(64\times 2^n - 24)}, \quad (44)$$

$$\mathrm{ENT}_{\sigma}(PyGn) = \log(72\times 2^n - 24) - \frac{(6243314768165359\times 2^n)}{281474976710656(72\times 2^n - 24)}. \quad (45)$$

Proof. To determine the entropy measures of $PyGn$, the similar pattern used in Theorem 5 is followed. The data from Theorem 6 and Table 4 are applied in Equation (5) in order to obtain the required degree-based graph entropy measures. □

5. Comparative Analysis

The numerical values computed for the distance- and degree-based descriptors of Gn upto the sixth generation and of $PyGn$ upto the fifth generation are presented in Tables 5–8. Further, the entropy measures computed for initial generations of the dendrimers are tabulated in Tables 9 and 10. A comparison between the descriptors and generations as well as between the entropies and generations of the dendrimers Gn and $PyGn$ are represented graphically in Figures 10–12.

6. QSPR/QSAR Modelling of Structural Descriptors

Theoretical structural descriptors are the numerical representation of chemical compounds, which encodes the structures topology and chemical information. There have been a number of molecular descriptors such as physicochemical, constitutional and geometrical, electrostatic, topological, and quantum chemical indices which are widely used in

Table 6: Computed numerical values of indices for initial generations of dendrimer *PyGn*.

Topological index	$n=0$	$n=1$	$n=2$	$n=3$	$n=4$	$n=5$
Wiener	8,226	71,242	472,674	2,719,858	14,368,146	71,798,482
Szeged	16,232	126,060	793,556	4,433,988	23,001,572	113,560,740
Edge Szeged	17,140	143,028	933,364	5,325,972	28,006,036	139,566,612
Padmakar–Ivan	2,912	14,900	66,620	281,036	1,153,772	4,674,860
Mostar	1,712	10,240	50,336	225,568	961,952	3,989,920
Edge Mostar	2,020	11,796	57,460	256,500	1,091,956	4,525,428

Table 7: Degree-based indices of *Gn* upto $n=6$.

Degree-based index	$n=1$	$n=2$	$n=3$	$n=4$	$n=5$	$n=6$
First Zagreb	558	1,486	3,342	7,054	14,478	29,326
Second Zagreb	709	1,885	4,237	8,941	18,349	37,165
Harmonic	45.333	120	269.333	568	1,165.333	2,360
Hyper Zagreb	2,876	7,660	17,228	36,364	74,636	151,180
Forgotten	1,458	3,890	8,754	18,482	37,938	76,850
Randić	45.6633	120.9897	271.6428	572.9490	1,175.5612	2,380.7857
Reciprocal Randić	276.9796	736.9388	1,656.8571	3,496.6938	7,176.3673	14,535.7142
Sum-connectivity	49.9937	132.6327	297.9107	628.4667	1,289.5786	2,611.8025
Geometric arithmetic	110.1918	292.5755	657.3429	1,386.8775	2,845.9469	5,764.0857
Atom bond connectivity	76.9926	204.8356	460.5216	971.8936	1,994.6376	4,040.1256
Irregularity and sigma	40	120	280	600	1,240	2,520

Table 8: Degree-based indices of *PyGn* upto $n=5$.

Degree-based index	$n=0$	$n=1$	$n=2$	$n=3$	$n=4$	$n=5$
First Zagreb	270	598	1,254	2,566	5,190	10,438
Second Zagreb	325	705	1,465	2,985	6,025	12,105
Harmonic	22.8	51.2	108	221.6	448.8	903.2
Hyper Zagreb	1,348	2,940	6,124	12,492	25,228	50,700
Forgotten	698	1,530	3,194	6,522	13,178	26,490
Randić	23.3733	52.5447	110.8873	227.5725	460.9429	927.6838
Reciprocal Randić	132.3119	292.4115	612.6108	1,253.0093	2,533.8063	5,095.4004
Sum-connectivity	24.9851	56.0290	118.1170	242.2928	490.6445	987.3479
Geometric arithmetic	53.8176	120.1502	252.8156	518.1463	1048.8076	2,110.1304
Atom bond connectivity	38.9645	87.4853	184.5269	378.6102	766.7768	1,543.1099
Irregularity measure	40	104	232	488	1,000	2,024
Sigma	48	120	264	552	1,128	2,280

quantitative structure–activity-property research for predicting biological activities and properties of chemicals. Quantitative structure–property relationships (QSPRs)/quantitative structure–activity relationships (QSARs) are the final results of a process that starts with a suitable descriptor of a molecular structure and ends with some inference, hypothesis and prediction on the behaviour, properties, and characteristics of the molecule. As an initial step, it is assumed that the molecule's structure has features responsible for some physical, chemical, and biological properties and the ability to capture these features into numerical descriptors, followed by gathering data regarding the molecules, which can be produced experimentally or retrieved from literature. A limiting factor at this step is the availability of high-quality experimental data and its accuracy. Another important phase of the QSPR/QSAR process is the selection of best structural descriptor for modelling in analysis. Since there is no awareness about the best among the molecular descriptors, all possible descriptors are determined.

A major application of QSPR/QSAR models is that the properties, activities, behaviour, etc., of a newly designed or untested chemical compound can be inferred from the

Table 9: Degree-based entropies of Gn upto $n = 6$.

Degree-based entropy	$n = 1$	$n = 2$	$n = 3$	$n = 4$	$n = 5$	$n = 6$
First Zagreb	4.6968	5.6752	6.4853	7.2323	7.9512	8.6569
Second Zagreb	4.6595	5.6405	6.4514	7.1987	7.9178	8.6237
Harmonic	4.6963	5.6746	6.4848	7.2316	7.9506	8.6564
Hyper Zagreb	4.6608	5.6420	6.4530	7.2002	7.9194	8.6253
Forgotten	4.6618	5.6430	6.4541	7.2014	7.9205	8.6264
Randić	4.6965	5.6748	6.4849	7.2318	7.9508	8.6566
Reciprocal Randić	4.6966	5.6750	6.4851	7.2320	7.9509	8.6568
Sum-connectivity	4.7062	5.6839	6.4938	7.2406	7.9595	8.6653
Geometric arithmetic	4.7095	5.6869	6.4967	7.2435	7.9624	8.6681
Atom bond connectivity	4.7091	5.6866	6.4964	7.2431	7.9621	8.6678
Irregularity and sigma	3.6889	4.7875	5.6348	6.3969	7.1229	7.8320

Table 10: Degree-based entropies of $PyGn$ upto $n = 5$.

Entropy	$n = 0$	$n = 1$	$n = 2$	$n = 3$	$n = 4$	$n = 5$
First Zagreb	3.9988	4.8065	5.5524	6.2709	6.9765	7.6758
Second Zagreb	3.9665	4.7849	5.5358	6.2567	6.9635	7.6635
Harmonic	3.9985	4.8061	5.5518	6.2703	6.9759	7.6752
Hyper Zagreb	3.9740	4.7903	5.5401	6.2605	6.9671	7.6668
Forgotten	3.9784	4.7930	5.5421	6.2621	6.9684	7.6681
Randić	3.9959	4.8039	5.5499	6.2685	6.9741	7.6734
Reciprocal Randić	3.9967	4.8049	5.5511	6.2697	6.9754	7.6747
Sum-connectivity	4.0051	4.8107	5.5556	6.2737	6.9791	7.6783
Geometric arithmetic	4.0067	4.8117	5.5564	6.2743	6.9796	7.6788
Atom bond connectivity	4.0062	4.8113	5.5561	6.2741	6.9794	7.6786
Irregularity measure	3.5503	4.5378	4.5378	6.0994	6.8190	7.5252
Sigma	3.4091	4.4178	5.2399	5.9921	6.7136	7.4206

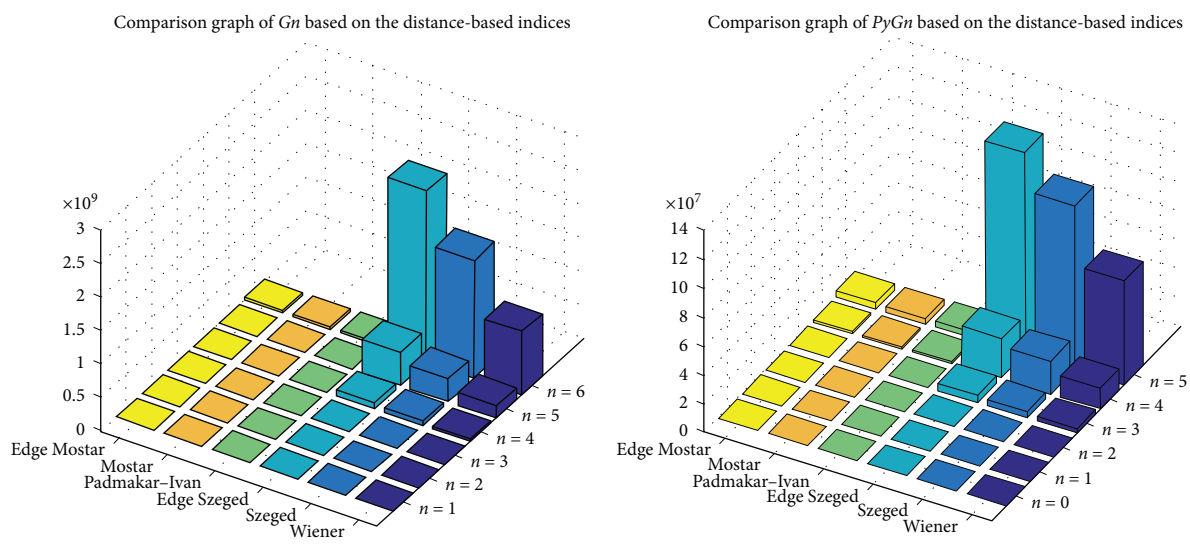

Figure 10: Comparison graph based on distance-based indices.

molecular structure of similar compounds whose properties, activities, characteristics, etc., have already been assessed. Researchers have done the analysis and they have highlighted their outcomes in [69–71].

A flowchart diagram is drawn based on the QSPR/QSAR modelling with respect to structural descriptors of chemical structures, especially with respect to dendrimers. The same is presented in Figure 13.

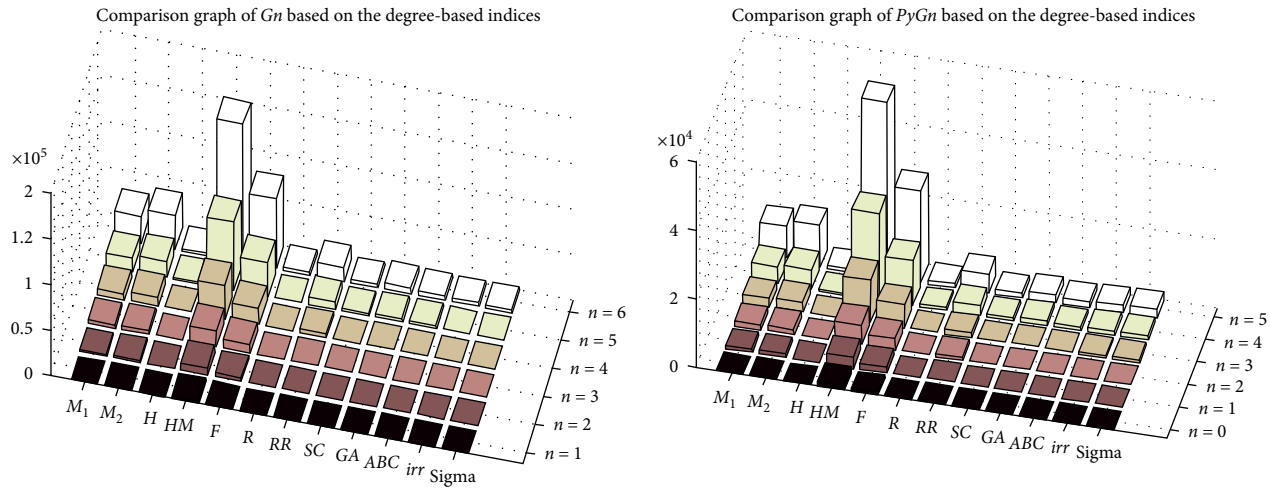

Figure 11: Comparison graph based on degree-based indices.

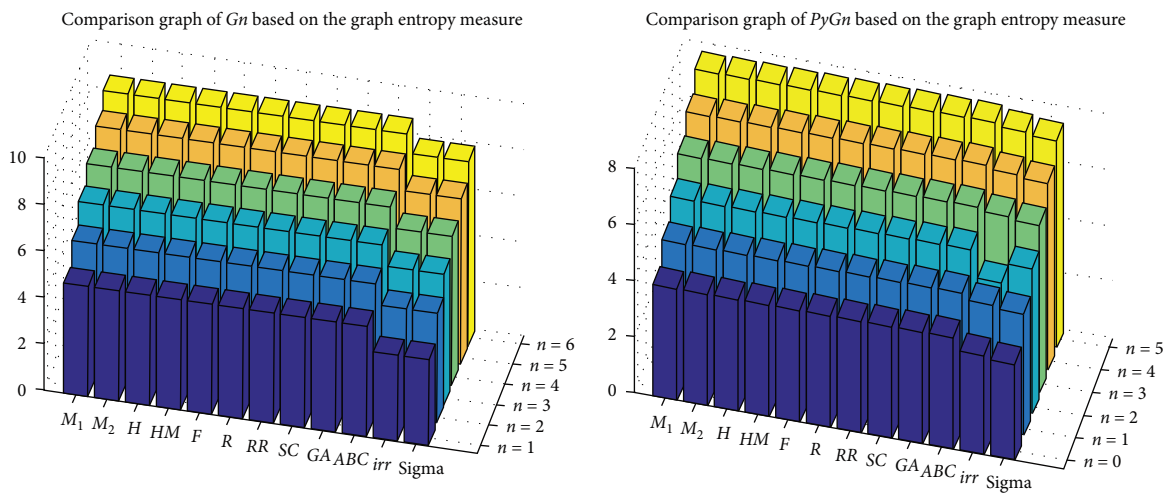

Figure 12: Comparison graph based on graph entropy measures.

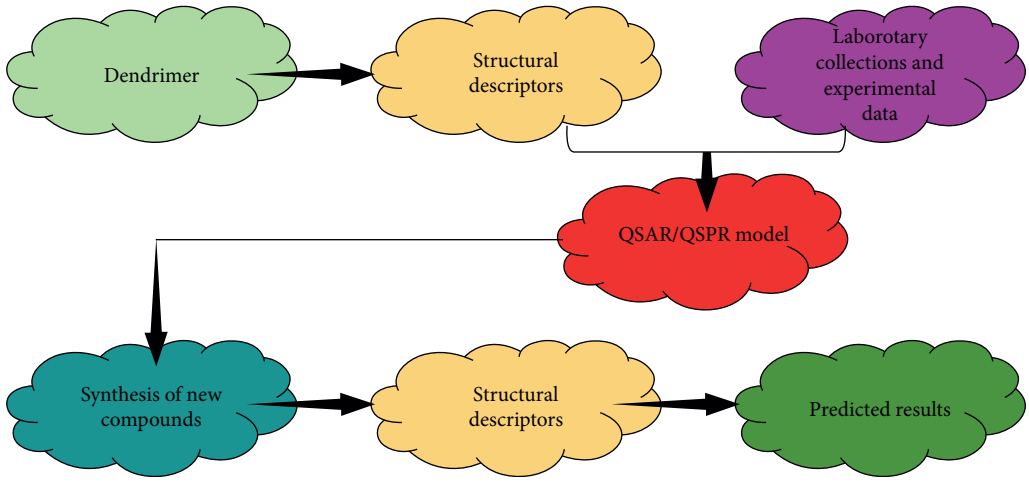

Figure 13: QSAR/QSPR flowchart model.

Table 11: Correlation coefficient ($\mathscr{R}$) between band gap energy of Gn and its descriptors.

Descriptor	$\mathscr{R}$
Wiener	−0.94484
Szeged	−0.94508
Edge Szeged	−0.94449
Padmakar–Ivan	−0.96186
Mostar	−0.95905
Edge Mostar	−0.95909
First Zagreb	−0.994191626
Second Zagreb	−0.994191626
Harmonic	−0.994191804
Hyper Zagreb	−0.994191626
Forgotten	−0.994191626
Randić	−0.994191573
Reciprocal Randić	−0.994191628
Sum-connectivity	−0.994191626
Geometric arithmetic	−0.994191626
Atom bond connectivity	−0.994191626
Irregularity	−0.994191626
Sigma	−0.994191626

6.1. Linear Regression Model for Descriptors of Pyrene Cored Dendrimers. In this section, the linear regression models for few properties of the pyrene cored dendrimers with their distance- and degree-based descriptors are obtained using least square procedure. The following regression model is considered for the analysis:

$$P = x(\mathrm{SD}) + y, \tag{46}$$

where P and SD stand for property and structural descriptor, respectively.

6.1.1. Linear Regression Model for the Structural Descriptors of Gn. The linear regression model for band gap energy of Gn with their distance- and degree-based descriptors is determined in this section. A band gap is defined as the energy difference between the upper edge of the valence band and the lower edge of the conduction band of a solid. The respective energy difference is called band gap energy (E_g). The band gap energy for $G1$, $G2$, and $G3$ are 2.92, 2.86, and 2.78, respectively, as given in You et al.'s [11] study. Analysing these data with respect to its corresponding descriptor value given in Tables 5 and 7, the correlation coefficients ($\mathscr{R}$) are determined and the same are presented in Table 11.

Based on the correlation coefficient ($\mathscr{R}$), the regression model for Padmakar–Ivan index, PI is found to be best fitted among the distance-based descriptors, which can be as follows:

$$P = -0.00003097(\mathrm{PI}) + 2.9065. \tag{47}$$

The regression model for Harmonic index, H is found to be best fitted among the degree-based descriptors and can be as follows:

$$P = -0.0006(H) + 2.942. \tag{48}$$

The scatter diagrams to show relation between property and descriptors are given in Figure 14.

6.1.2. Linear Regression Model for the Structural Descriptors of PyGn. The linear regression model for band emission of $PyGn$ with their distance- and degree-based descriptors is determined in this section. Band emission is the fraction of the total emission from a blackbody that is in a certain wavelength interval or band. The emission bands for first three dendrimer generations in $CHCl_3$ solutions strongly red-shifted with maximum at 448 nm for $PyG0$, 452 nm for $PyG1$, and 457 nm for $PyG2$ [72]. Analysing these data with respect to its corresponding descriptor value given in Tables 6 and 8, the correlation coefficients are determined and presented in Table 12.

Based on the correlation coefficient ($\mathscr{R}$), the regression model for Padmakar–Ivan index, PI is found to be best fitted among the distance-based descriptors and can be as follows:

$$P = 0.0001(\mathrm{PI}) + 448.73. \tag{49}$$

The regression model for Randić index, R is found to be best fitted among the degree-based descriptors and can be as follows:

$$P = 0.1004(R) + 446.08. \tag{50}$$

The scatter diagrams to show relation between property and descriptors are given in Figure 15.

Thus, it can be concluded that the abovementioned properties of the pyrene cored dendrimers can be predicted with the help of regression equations using the computed structural descriptors.

7. Discussion

We have computed the numerical values of the distance- and degree-based descriptors for the initial generation dendrimer structures. Also, the entropy for Gn and $PyGn$ was also computed using the determined expressions. Based on the obtained values, a comparison between the descriptors and generations as well as between the entropies and generations of the dendrimers Gn and $PyGn$ are presented graphically in Section 5. The numerical computations and plotting of the comparison graphs were prepared with the help of MATLAB software. A regression analysis was also performed based on a few dendrimer structure properties, and the best fit regression models were identified and are presented in Section 6. Microsoft Excel analysis tools were used for the regression analysis.

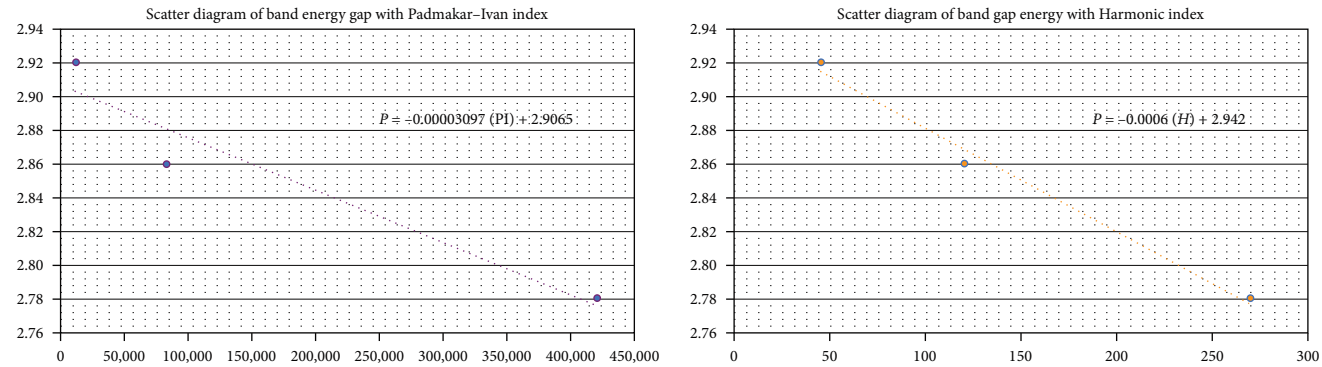

Figure 14: Scatter diagram for band energy gap with descriptors of pyrene cored dendrimer, *Gn*.

Table 12: Correlation coefficient ($\mathscr{R}$) between band emission of *PyGn* and its descriptors.

Descriptor	$\mathscr{R}$
Wiener	0.94469
Szeged	0.94649
Edge Szeged	0.94524
Padmakar–Ivan	0.96062
Mostar	0.95693
Edge Mostar	0.95721
First Zagreb	0.992064533
Second Zagreb	0.992064533
Harmonic	0.992064533
Hyper Zagreb	0.992064533
Forgotten	0.992064533
Randić	0.99206464
Reciprocal Randić	0.992064523
Sum-connectivity	0.992064433
Geometric arithmetic	0.992064486
Atom bond connectivity	0.970998101
Irregularity	0.992064533
Sigma	0.992064533

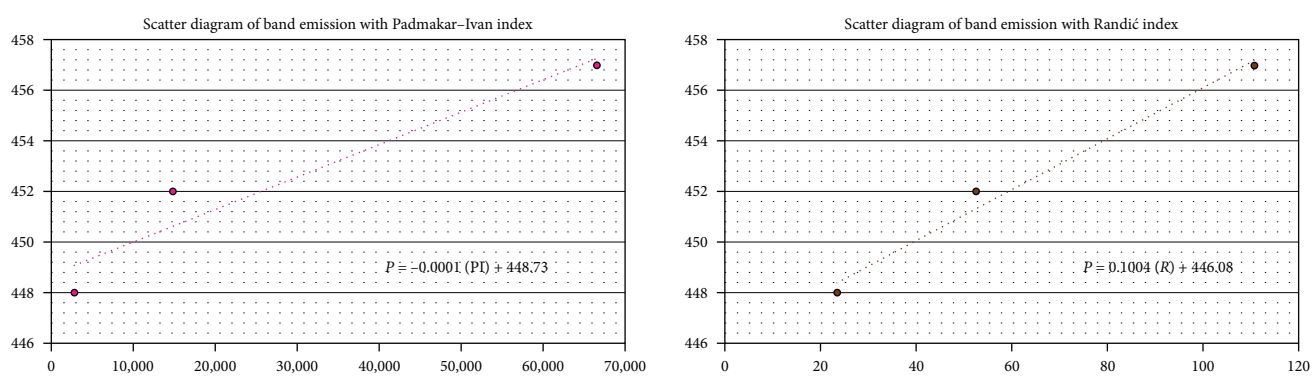

Figure 15: Scatter diagram for band emission with descriptors of pyrene cored dendrimer, *PyGn*.

8. Conclusion

The distance-based descriptors of pyrene cored dendrimers $Gn : n \geq 1$ and $PyGn : n \geq 0$ are computed by transforming the original graph into quotient graphs. The degree-based descriptors for the pyrene cored dendrimers Gn and $PyGn$ are also discussed, for which the degree counting method and edge partition based on the vertices and edges are used. Further, the degree-based entropy measures were determined for the dendrimer structures using Shannon's method. These values are related to different physical, chemical, and biological properties of the dendrimers, which has wide range of application in disparate fields. The determined topological descriptors and the entropy values can be used to predict the physicochemical, thermochemical, electrical, mechanical, and optical properties of the structures. Also, this work would be useful in QSPR and QSAR analysis of these hyperbranched nanomaterials. Further, it may help in developments and recognitions in the field of macromolecules and in deriving its properties and applications.

Data Availability

All the data and material used in this research are included in the paper.

Conflicts of Interest

The authors declare that they have no conflicts of interest.

References

[1] D. A. Tomalia and J. M. J. Fréchet, "Discovery of dendrimers and dendritic polymers: a brief historical perspective," *Journal of Polymer Science Part A: Polymer Chemistry*, vol. 40, no. 16, pp. 2719–2728, 2002.

[2] E. Abbasi, S. F. Aval, A. Akbarzadeh et al., "Dendrimers: synthesis, applications, and properties," *Nanoscale Research Letters*, vol. 9, no. 1, pp. 1–10, 2014.

[3] F. Zeng and S. C. Zimmerman, "Dendrimers in supramolecular chemistry: from molecular recognition to self-assembly," *Chemical Reviews*, vol. 97, no. 5, pp. 1681–1712, 1997.

[4] S. R. Shahi, M. S. Kulkarni, G. S. Karva, P. S. Giram, and R. R. Gugulkar, "Dendrimers," *International Journal of Pharmaceutical Sciences Review and Research*, vol. 33, no. 1, pp. 187–198, 2015.

[5] A. Samad, M. Alam, and K. Saxena, "Dendrimers: a class of polymers in the nanotechnology for the delivery of active pharmaceuticals," *Current Pharmaceutical Design*, vol. 15, no. 25, pp. 2958–2969, 2009.

[6] D. Huang and D. Wu, "Biodegradable dendrimers for drug delivery," *Materials Science and Engineering: C*, vol. 90, pp. 713–727, 2018.

[7] M. Liu and J. M. J. Fréchet, "Designing dendrimers for drug delivery," *Pharmaceutical Science & Technology Today*, vol. 2, no. 10, pp. 393–401, 1999.

[8] J.-P. Majoral, A.-M. Caminade, R. Laurent, and P. Sutra, "Phosphorus-containing dendrimers: from material science to biology," *Heteroatom Chemistry*, vol. 13, no. 5, pp. 474–485, 2002.

[9] S. Langereis, A. Dirksen, T. M. Hackeng, M. H. P. van Genderen, and E. W. Meijer, "Dendrimers and magnetic resonance imaging," *New Journal of Chemistry*, vol. 31, no. 7, pp. 1152–1160, 2007.

[10] M. Irfan, A. Saeed, S. Akram, and S. bin Yameen, "Dendrimers chemistry and applications: a short review," *Frontiers in Chemical Sciences*, vol. 1, no. 1, pp. 29–40, 2020.

[11] J. You, G. Li, and Z. Wang, "Synthesis of pyrene-cored dendrimers with 9-phenylcarbazole-based dendrons and their thermal, photophysical and electrochemical properties," *Polymer*, vol. 53, no. 22, pp. 5116–5123, 2012.

[12] J. You, G. Li, R. Wang, Q. Nie, Z. Wang, and J. Li, "Pyrene-cored dendrimer with carbazole derivatives as dendrons: synthesis, properties and application in white light-emitting diode," *Physical Chemistry Chemical Physics*, vol. 13, no. 39, pp. 17825–17830, 2011.

[13] M. Gingras, V. Placide, J.-M. Raimundo, G. Bergamini, P. Ceroni, and V. Balzani, "Polysulfurated pyrene-cored dendrimers: luminescent and electrochromic properties," *Chemistry—A European Journal*, vol. 14, no. 33, pp. 10357–10363, 2008.

[14] G. Valenti, A. Fiorani, S. Di Motta et al., "Molecular size and electronic structure combined effects on the electrogenerated chemiluminescence of sulfurated pyrene-cored dendrimers," *Chemistry—A European Journal*, vol. 21, no. 7, pp. 2936–2947, 2015.

[15] H. Wiener, "Structural determination of paraffin boiling points," *Journal of the American Chemical Society*, vol. 69, no. 1, pp. 17–20, 1947.

[16] S. S. Asghar, M. A. Binyamin, Y.-M. Chu, S. Akhtar, and M. A. Malik, "Szeged-type indices of subdivision vertex-edge join (SVE-join)," *Main Group Metal Chemistry*, vol. 44, no. 1, pp. 82–91, 2021.

[17] A. T. Balaban, *Chemical Applications of Graph Theory*, Academic Press, 1976.

[18] I. Gutman and N. Trinajstić, "Graph theory and molecular orbitals. Total ϕ-electron energy of alternant hydrocarbons," *Chemical Physics Letters*, vol. 17, no. 4, pp. 535–538, 1972.

[19] J.-B. Liu, H. M. A. Siddiqui, M. F. Nadeem, and M. A. Binyamin, "Some topological properties of uniform subdivision of Sierpiński graphs," *Main Group Metal Chemistry*, vol. 44, no. 1, pp. 218–227, 2021.

[20] M. Randic, "Characterization of molecular branching," *Journal of the American Chemical Society*, vol. 97, no. 23, pp. 6609–6615, 1975.

[21] M. Randić, "Novel molecular descriptor for structure–property studies," *Chemical Physics Letters*, vol. 211, no. 4-5, pp. 478–483, 1993.

[22] S. Shirakol, M. Kalyanshetti, and S. M. Hosamani, "QSPR analysis of certain distance based topological indices," *Applied Mathematics and Nonlinear Sciences*, vol. 4, no. 2, pp. 371–386, 2019.

[23] C. E. Shannon, "A mathematical theory of communication," *Bell System Technical Journal*, vol. 27, no. 3, pp. 379–423, 1948.

[24] D. S. Sabirov and I. S. Shepelevich, "Information entropy in chemistry: an overview," *Entropy*, vol. 23, no. 10, Article ID 1240, 2021.

[25] A. Mowshowitz and M. Dehmer, "Entropy and the complexity of graphs revisited," *Entropy*, vol. 14, no. 3, pp. 559–570, 2012.

[26] N. Rashevsky, "Life, information theory, and topology," *The Bulletin of Mathematical Biophysics*, vol. 17, no. 3, pp. 229–235, 1955.

[27] M. P. Rahul, J. Clement, J. S. Junias, M. Arockiaraj, and K. Balasubramanian, "Degree-based entropies of graphene,

graphyne and graphdiyne using Shannon's approach," *Journal of Molecular Structure*, vol. 1260, Article ID 132797, 2022.

[28] A. Baby, K. Julietraja, and D. A. Xavier, "On molecular structural characterization of cyclen cored dendrimers," *Polycyclic Aromatic Compounds*, pp. 1–23, 2023.

[29] Y. Bashir, A. Aslam, M. Kamran et al., "On forgotten topological indices of some dendrimers structure," *Molecules*, vol. 22, no. 6, Article ID 867, 2017.

[30] S. M. Kang, M. A. Zahid, Aur R. Virk, W. Nazeer, and W. Gao, "Calculating the degree-based topological indices of dendrimers," *Open Chemistry*, vol. 16, no. 1, pp. 681–688, 2018.

[31] M. Munir, W. Nazeer, S. Rafique, and S. Kang, "M-polynomial and related topological indices of nanostar dendrimers," *Symmetry*, vol. 8, no. 9, Article ID 97, 2016.

[32] D. A. Xavier, S. Akhila, A. Alsinai et al., "Distance-based structure characterization of PAMAM-related dendrimers nanoparticle," *Journal of Nanomaterials*, vol. 2022, Article ID 2911196, 16 pages, 2022.

[33] D. A. Xavier, K. Julietraja, and A. T. Nair, "Distance based structural descriptors of non-conjugated ethylene oxide dendritic core decorated with tetraphenylethylene," *Polycyclic Aromatic Compounds*, 2023.

[34] M. Arockiaraj, J. Clement, and K. Balasubramanian, "Topological indices and their applications to circumcised donut benzenoid systems, kekulenes and drugs," *Polycyclic Aromatic Compounds*, vol. 40, no. 2, pp. 280–303, 2020.

[35] M. Arockiaraj, S. Prabhu, M. Arulperumjothi, S. R. J. Kavitha, and K. Balasubramanian, "Topological characterization of hexagonal and rectangular tessellations of kekulenes as traps for toxic heavy metal ions," *Theoretical Chemistry Accounts*, vol. 140, no. 4, Article ID 43, 2021.

[36] I. Gutman, "Degree-based topological indices," *Croatica Chemica Acta*, vol. 86, no. 4, pp. 351–361, 2013.

[37] S. Fajtlowicz, "On Conjectures of Grafitti II," *Congressus Numerantium*, vol. 60, pp. 189–197, 1987.

[38] G. H. Shirdel, H. Rezapour, and A. M. Sayadi, "The hyper-zagreb index of graph operations," *Iranian Journal of Mathematical Chemistry*, vol. 4, no. 2, pp. 213–220, 2013.

[39] B. Furtula and I. Gutman, "A forgotten topological index," *Journal of Mathematical Chemistry*, vol. 53, no. 4, pp. 1184–1190, 2015.

[40] O. Favaron, M. Mahéo, and J.-F. Saclé, "Some eigenvalue properties in graphs (conjectures of Graffiti-II)," *Discrete Mathematics*, vol. 111, no. 1–3, pp. 197–220, 1993.

[41] B. Zhou and N. Trinajstić, "On general sum-connectivity index," *Journal of Mathematical Chemistry*, vol. 47, no. 1, pp. 210–218, 2010.

[42] D. Vukičević and B. Furtula, "Topological index based on the ratios of geometrical and arithmetical means of end-vertex degrees of edges," *Journal of Mathematical Chemistry*, vol. 46, no. 4, pp. 1369–1376, 2009.

[43] E. Estrada, L. Torres, L. Rodriguez, and I. Gutman, "An atom-bond connectivity index: modelling the enthalpy of formation of alkanes," 1998.

[44] M. O. Albertson, "The irregularity of a graph," *Ars Combinatoria*, vol. 46, pp. 219–225, 1997.

[45] I. Gutman, M. Togan, A. Yurttas, A. S. Cevik, and I. N. Cangul, "Inverse problem for sigma index," *MATCH Communications in Mathematical and in Computer Chemistry*, vol. 79, no. 2, pp. 491–508, 2018.

[46] S. Govardhan and S. Roy, "Topological analysis of hexagonal and rectangular porous graphene with applications to predicting π-electron energy," *The European Physical Journal Plus*, vol. 138, no. 7, Article ID 670, 2023.

[47] J. S. Junias and J. Clement, "Predictive analytics of conductance and HOMO-LUMO gaps with topological descriptors of porphyrin nanosheets," *Physica Scripta*, vol. 99, no. 1, Article ID 015208, 2023.

[48] M. P. Rahul and J. Clement, "Topological characterization and entropy measures of large cavity cycloarene oligomers," *The European Physical Journal Plus*, vol. 137, no. 12, Article ID 1365, 2022.

[49] M. P. Rahul and J. Clement, "QSPR analysis of carbon allotropes by employing molecular descriptors and information entropies," *Ain Shams Engineering Journal*, vol. 14, no. 11, Article ID 102542, 2023.

[50] P. N. A. D. Renai and S. Roy, "On computation of degree based entropy measures for terpyridine complex nanosheet," *International Journal of Quantum Chemistry*, vol. 123, no. 20, Article ID e27190, 2023.

[51] S. Amin, A. Ur Rehman Virk, M. A. Rehman, and N. A. Shah, "Analysis of dendrimer generation by sombor indices," *Journal of Chemistry*, vol. 2021, Article ID 9930645, 11 pages, 2021.

[52] J. C. Dearden, "The use of topological indices in QSAR and QSPR modeling," in *Advances in QSAR Modeling*, vol. 24 of *Challenges and Advances in Computational Chemistry and Physics*, pp. 57–88, Springer, Cham, 2017.

[53] S. Hayat, "Distance-based graphical indices for predicting thermodynamic properties of benzenoid hydrocarbons with applications," *Computational Materials Science*, vol. 230, Article ID 112492, 2023.

[54] S. Hayat, M. Imran, and J.-B. Liu, "An efficient computational technique for degree and distance based topological descriptors with applications," *IEEE Access*, vol. 7, pp. 32276–32296, 2019.

[55] S. Hayat, S. Khan, A. Khan, and M. Imran, "Distance-based topological descriptors for measuring the π-electronic energy of benzenoid hydrocarbons with applications to carbon nanotubes," *Mathematical Methods in the Applied Sciences*, 2020.

[56] S. Hayat, S. Khan, A. Khan, and J. B. Liu, "Valency-based molecular descriptors for measuring the π-electronic energy of lower polycyclic aromatic hydrocarbons," *Polycyclic Aromatic Compounds*, vol. 42, no. 4, pp. 1113–1129, 2022.

[57] S. Hayat, N. Suhaili, and H. Jamil, "Statistical significance of valency-based topological descriptors for correlating thermodynamic properties of benzenoid hydrocarbons with applications," *Computational and Theoretical Chemistry*, vol. 1227, Article ID 114259, 2023.

[58] S. A. K. Kirmani, P. Ali, and J. Ahmad, "Topological coindices and quantitative structure-property analysis of antiviral drugs investigated in the treatment of COVID-19," *Journal of Chemistry*, vol. 2022, Article ID 3036655, 15 pages, 2022.

[59] M. Y. H. Malik, M. A. Binyamin, and S. Hayat, "Correlation ability of degree-based topological indices for physicochemical properties of polycyclic aromatic hydrocarbons with applications," *Polycyclic Aromatic Compounds*, vol. 42, no. 9, pp. 6267–6281, 2022.

[60] M. Mohammadi, H. Barzegar, and A. R. Ashrafi, "Comparisons of the sombor index of alkane, alkyl, and annulene series with their molecular mass," *Journal of Chemistry*, vol. 2022, Article ID 8348525, 7 pages, 2022.

[61] I. Redžepović, "Chemical applicability of Sombor indices," *Journal of the Serbian Chemical Society*, vol. 86, no. 5, pp. 445–457, 2021.

[62] J. A. Bondy and U. S. R. Murty, *Graph Theory with Applications*, Vol. 290, Macmillan, London, 1976.

[63] R. Kazemi, "Entropy of weighted graphs with the degree-based topological indices as weights," *MATCH Communications in Mathematical and in Computer Chemistry*, vol. 76, no. 1, pp. 69–80, 2016.

[64] M. Arockiaraj, S. Klavžar, S. Mushtaq, and K. Balasubramanian, "Distance-based topological indices of nanosheets, nanotubes and nanotori of SiO_2," *Journal of Mathematical Chemistry*, vol. 57, pp. 343–369, 2019.

[65] S. Klavžar, P. Manuel, M. J. Nadjafi-Arani, R. S. Rajan, C. Grigorious, and S. Stephen, "Average distance in interconnection networks via reduction theorems for vertex-weighted graphs," *The Computer Journal*, vol. 59, no. 12, pp. 1900–1910, 2016.

[66] S. Klavžar and M. J. Nadjafi-Arani, "Wiener index in weighted graphs via unification of Θ^*-classes," *European Journal of Combinatorics*, vol. 36, pp. 71–76, 2014.

[67] D. A. Xavier, E. S. Varghese, A. Baby, D. Mathew, and M. K. A. Kaabar, "Distance based topological descriptors of zinc porphyrin dendrimer," *Journal of Molecular Structure*, vol. 1268, Article ID 133614, 2022.

[68] I. Rajasingh, P. Manuel, N. Parthiban, D. A. Jemilet, and R. S. Rajan, "Transmission in butterfly networks," *The Computer Journal*, vol. 59, no. 8, pp. 1174–1179, 2016.

[69] S. A. K. Kirmani, P. Ali, and F. Azam, "Topological indices and QSPR/QSAR analysis of some antiviral drugs being investigated for the treatment of COVID-19 patients," *International Journal of Quantum Chemistry*, vol. 121, no. 9, Article ID e26594, 2021.

[70] S. Nandi and M. C. Bagchi, "QSAR of aminopyrido[2,3-d] pyrimidin-7-yl derivatives: anticancer drug design by computed descriptors," *Journal of Enzyme Inhibition and Medicinal Chemistry*, vol. 24, no. 4, pp. 937–948, 2009.

[71] S. Nandi and T. Sharma, "QSAR of 1, 3, 5-triazine compounds towards inhibition of toxoplasmosis utilizing computed molecular descriptors," *Indian Journal of Chemistry-Section B (IJC-B)*, vol. 59, no. 12, pp. 1881–1886, 2020.

[72] J. Y. Hu and T. Yamato, "Synthesis and photophysical properties of pyrene-based multiply conjugated shaped light-emitting architectures," in *Organic Light Emitting Diode Material, Process and Devices*, pp. 22–54, IntechOpen, 2011.